



JIMMA UNIVERSITY

JIMMA INSTITUTE OF TECHNOLOGY

FACULTY OF ELECTRICAL AND COMPUTER ENGINEERING

**Design and Analysis of Slotted Ground Plane and Slotted Patch Micro strip Antenna
Arrays for Wireless Communications**

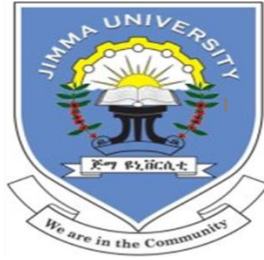
**A thesis report submitted to the school of graduate studies
of Jimma University in partial fulfillment of the
requirements for the degree of Masters of Science in
Communication Engineering**

By :

Amsalu Abera

Jimma, Ethiopia

February 2, 2022



JIMMA UNIVERSITY

JIMMA INSTITUTE OF TECHNOLOGY (JIT)

FACULTY OF ELECTRICAL AND COMPUTER ENGINEERING

(COMMUNICATION ENGINEERING STREAM)

**Design and Analysis of Slotted Ground Plane and Slotted Patch Microstrip
Antenna Arrays for Wireless Communications**

**A thesis report submitted to the school of graduate studies
of Jimma University in partial fulfillment of the
requirements for the degree of Masters of Science in
Communication Engineering**

By :

Amsalu Abera

Main-Advisor:Dr.Kinde Anlay

CO-Advisor: Mr.Sherwin Catolos(Ing)

Jimma,Ethiopia

Febraury 2,2022

Dedication

I dedicate this thesis to my close friend ,**Fkadu Gebre** whom I lost during the season of this study.May his soul Rest in Peace.

Declaration

I, the undersigned, declare that this thesis is my original work and has not been presented for a degree in this and any other Universities, and all sources of materials used for the thesis have been fully acknowledged.

Submitted by: Amsalu Abera _____

Name


Signature

Date

Place: Jimma

Approved by Advisors

Dr. Kinde Anlay



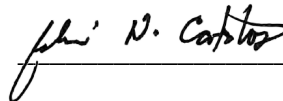
11/03/2022

Advisor's name

Signature

Date

Mr. Sherwin Catolos



14/03/2022

Co-advisor's name

Signature

Date

Approved by faculty of Electrical and Computer Engineering research thesis examination members

1. Dr. Yihenew Wondie



11/03/2022

External Examiner

Signature

Date

2. _____

Internal Examiner

Signature

Date

3. _____

Chairman

Signature

Date

Abstract

Micro strip patch antennas are playing an important role in wireless communication systems because of their many advantages, like light weight, low profile, low cost, easy integration with planar structures, and easy fabrication. So, it is very essential to know all the aspects of micro strip antennas. The main objective of this thesis is to discuss the design and analysis issues of slotted ground plane and slotted patch micro strip array antennas. The design issues include single element antenna dimensions, feeding techniques, and antenna arrays, whereas the analysis issues include return loss, bandwidth, directivity, and radiation pattern of slotted microstrip patch array antennas. In this thesis, a slotted rectangular patch antenna and an array antenna for wireless communication have been proposed. By developing wide bandwidth characteristics, long ranges of data transfer are covered with better quality of signal transmission in the communication system. The creation of slots in both patch and ground plane structures has influenced the frequency bandwidth. The design, analysis, and optimization of the proposed work along with parametric analysis were performed using CST Microwave Studio 2019. A slotted micro strip patch antenna has been designed at a millimeter wave for consistent radiation patterns and higher gain at operating frequency. A Rogers RT/Duriod-5880 substrate has been employed in this work with a dielectric constant value of 2.2, a thickness value of 0.254 mm, and a loss tangent value of 0.0009. The proposed single-element slotted rectangular patch antenna has achieved a wider bandwidth which is 23.858 GHz with a return loss of -46.294dB at the center frequency of 28.001 GHz, a VSWR of 1.009 at 28.001 GHz, and a maximum gain of 7.27 dBi with high directivity of 7.65 dBi at 28.001 GHz, and a 4x1 slotted array antenna has achieved high gain and directivity which is 12.9 dBi and 13.9 dBi at the center frequency of 28.222 GHz. The single slotted antenna results of this work were shown to be useful in fulfilling the requirements of wider bandwidth, and slotted 4x1 antenna arrays offer higher gain and directivity for wireless communications.

Keywords: Bandwidth, Gain, CST, Return loss, VSWR, Rogers RT/Duriod.

Acknowledgement

I would like to express my appreciation and give a special thanks to my advisor, **Dr. Kinde Anlay**, for his giving time, patience, understanding and continual guidance in my work.

Next, I am pleased to forward my heartfelt gratitude to Mr. Sherwin Catalos (Ing), co-advisor, and Mrs. Sofia Ali, chairperson of the communication engineering stream, for their valuable advice and guidance.

I would like to express my sincerest gratitude to the Hossana Town Municipality Administration for offering me the chance to continue in my academic career. Last but not least, I would like to extend my gratitude to all my family members and co-workers, Mr. Afework Tadese, Mr. Amanuel Admassu, Mrs. Hawi Hailu, and Mrs. Arebe Husen, for their courage, patience, and advice.

Table of Contents

Dedication	III
Declaration.....	IV
Abstract.....	V
Acknowledgement	VI
List of Tables	X
List of Figures.....	XI
List of Acronyms and Abbreviations	XIII
List of Symbols	XIV
1. Introduction.....	1
1.1 Background	1
1.2 Motivation.....	4
1.3 Statement of Problem.....	5
1.3 Objectives	6
1.3.1 General objective	6
1.3.2 Specific objectives	6
1.4 Significance of the Study	7
1.5 Scope and limitations of the study	8
1.6 Methodology	9
1.7 Contribution	11
1.8 Thesis Organization	12
2. Literature Review and Antenna Theory.....	13
2.1 Introduction to Antenna Theory.....	13
2.2 Antenna Fundamentals.....	15
2.2.1 Input Impedance.....	15
2.2.2 Voltage Standing Wave Ratio.....	15
2.2.3 Return Loss	16
2.2.4 Antenna Efficiency	16
2.2.5 Gain.....	17
2.2.6 Bandwidth.....	18
2.2.7 Radiation Pattern.....	18

2.3 Related Work	20
3. Micro strip Patches Antenna	23
3.1 Introduction.....	23
3.2 Advantages and Disadvantages of MSPA	25
3.3 Antenna Feeding Techniques.....	25
3.3.1 Probe feed	25
3.3.2 Microstrip feeds	25
3.3.3 Aperture coupling feed.....	26
3.3.4 Coupled Indirect Feed.....	27
3.4 Micro strips Array	27
3.4.1 The Array Factor for Linear Arrays	28
3.5 Antenna Array feeding Configuration	31
3.5.1 Parallel Feed.....	31
3.5.2 Series Feed	32
3.6 Mutual coupling	33
3.6.1 Introduction.....	33
3.6.2 Mutual Coupling in Antenna Array	34
3.6.3 Reduction of Mutual Coupling	34
4. Design of Single Element and 4x1 Slotted MSPA.....	35
4.1 Introduction.....	35
4.2 Design Specifications.....	35
4.3 Design Equations of MSPA	36
4.3.1 Patch dimensions Calculations (W_p and L_p).....	36
4.3.2 Ground plane dimensions calculation (L_g and W_g)	37
4.3.3 The Feed line calculation	37
4.3.4 Array Calculation.....	38
4.3.5 Calculation of the Impedance for Quarter-Wave Transformer	39
4.4 Antenna Design-2	41
4.5 Antenna Design-3	42
4.6 Design of the Proposed Antenna.....	44
4.5 Design of 2x1 slotted rectangular MSPA Arrays.....	45
4.5 Design of 4x1 slotted rectangular MSPA Arrays.....	47

5. Simulation results and Discussion	50
5.1 Introduction.....	50
5.2 Antenna Design-1 Simulation Results	50
5.3 Antenna Design-2 Simulation Results	53
5.4 Antenna Design-3 Simulation Results	57
5.5 Design of the Proposed Antenna-4 Simulation Results	61
5.6: Proposed 2×1 slotted antenna arrays.....	63
5.6: 4×1 slotted antenna arrays	65
5.7 Comparisons between Proposed Antennas and existing Work.....	68
6. Conclusion and Future work.....	70
6.1 Conclusion	70
6.2 Future work.....	71
References.....	72

List of Tables

Table 4. 1: Single Patch Antenna Design Specifications.....	36
Table 4. 2: Design parameters of Antenna Design-1.....	41
Table 4. 3: Design parameters of Antenna Design-2.....	42
Table 4. 4: Design parameters of the Antenna Design-3.....	43
Table 4. 5: Design parameters of the proposed antenna.....	45
Table 4. 6: Dimension of 2x1 Rectangular Patches Array Antenna.....	46
Table 4. 7: Dimension of Rectangular Patches Array Antenna.....	48
Table 5. 1: Comparison of proposed antenna-4 and 4x1 arrays with existing works.....	69

List of Figures

Figure 1. 1: Flow chart of methodology	10
Figure 2. 1: The antenna as a transition region between guided and propagating waves [6]	13
Figure 2. 2: Transmission line equivalent circuit of antenna in transmitting mode [6]	14
Figure 2. 3: Concept of an Antenna's Gain	17
Figure 2. 4: 3D Radiation Pattern	19
Figure 2. 5: 2D radiation Pattern.....	19
Figure 2. 6: Half Power Beamwidth	19
Figure 3. 1: Rectangular Patch Antenna [6].....	23
Figure 3. 2: Common Available Shape of Micro strip Antenna [21]	24
Figure 3. 3: Coaxial Probe Feed	25
Figure 3. 4: 2D View of Microstrip Transmission Line Feed.....	26
Figure 3. 5: Aperture Coupling.....	27
Figure 3. 6: Coupled Indirect Feed	27
Figure 3. 7:A typical linear array [56].	29
Figure 3. 8: Equivalent configuration of the array[56]	30
Figure 3. 9: Equally spaced linear array of isotropic point sources [56].	30
Figure 3. 10: Array radiation pattern [55].....	31
Figure 3. 11: Configurations of parallel feed microstrip array [6].	32
Figure 3. 12: Configurations of series feed microstrip array	33
Figure 4. 1: Rectangular Microstrip patch antenna.....	35
Figure 4. 2: Four Elements Array Line Impedance Design Layout.....	38
Figure 4. 3: Antenna Design-1	40
Figure 4. 4: Antenna Design-2 (a) Front view and (b) Back view	41
Figure 4. 5: Antenna Design-3 (a) Front View and (b) Back View.....	43
Figure 4. 6: Proposed of the proposed antenna where (a) front view and (b) back view	44
Figure 4. 7: 2 x 1 array of slotted antenna (a) front view and (b) back view.....	46
Figure 4. 8a: Constructional Details of 4 x 1 array of front view	47
Figure 4. 8b: Constructional Details of 4 x 1 array of ground plane	48
Figure 5. 1: Reflection Coefficient of Antenna Design-1	51
Figure 5. 2: VSWR of Antenna Design-1	51

Figure 5. 3a: 3D Radiation Pattern of Antenna Design-1	52
Figure 5. 4b: 2D Radiation Pattern of Antenna Design-1	53
Figure 5. 5: Reflection Coefficient of Antenna Design-2.....	54
Figure 5. 6: VSWR of Antenna Design-2.....	54
Figure 5. 7a: 3D Radiation Pattern of Antenna Design-2.....	55
Figure 5. 8a: 2D Radiation Pattern of Antenna Design-2.....	56
Figure 5. 9: Reflection Coefficient of Antenna Design-3.....	58
Figure 5. 10: VSWR of Antenna Design-3.....	58
Figure 5. 11a: 3D Radiation Pattern of Antenna Design-3.....	59
Figure 5. 12a: 2D Radiation Pattern of Antenna Design-3.....	60
Figure 5. 13: Reflection Coefficient of ProposedAntenna-4	61
Figure 5. 14: VSWR of ProposedAntenna-4	62
Figure 5. 15a: 3D Radiation Pattern of Proposed Antenna Design-4	62
Figure 5. 16: Reflection Coefficient of Proposed 2x1 arrays	63
Figure 5. 17a: 3D Radiation Pattern of Proposed 2x1 array	64
Figure 5. 18a: 2D Radiation Pattern of Proposed 2x1 array	65
Figure 5. 19: Reflection Coefficient of Proposed 4x1 arrays	66
Figure 5. 20a: 3D Radiation Pattern of Proposed 4x1 array	66
Figure 5. 21b: 2D Radiation Pattern of Proposed 4x1 array.....	67

List of Acronyms and Abbreviations

AF	Array factor
BW	Bandwidth
CST	Computer Simulation Technology
CM	Cavity model
DGS	Defected Ground Structure
FBW	Fractional Bandwidth
FEM	Finite element method
FDTD	Finite difference time domain
HPBW	Half Power Beamwidth
IEEE	Institute of Electrical and Electronics Engineers
IMT	International Mobile Telecommunications
ISI	Inter-Symbol Interface
ITU	International Telecommunication Union
MIMO	Multiple Input Multiple Output
MSPA	Micro strip Patch Antenna
PL	Path Loss
RF	Radio Frequency
S11	Reflection Coefficient in dB
SNR	Signal to Noise Ratio
TL	Transmission line model
VSWR	Voltage standing wave ratio

List of Symbols

C	Speed of light
μ_0	Permittivity
ε	Effective permittivity
e_0	Total efficiency
e_r	Reflection (mismatch)
e_c	Conduction efficiency
e_d	Dielectric efficiency
λ_0	Free space wavelength
f_C	Center frequency
f_H	High frequency
f_L	Low frequency
h	Thickness of substrate
L_p	Length of patch
L_{eff}	Effective length
ΔL	Delta length
W_p	Width of patch
W_{eff}	Effective width
Γ	Reflection coefficient
V_0^-	Reflected voltage
V_0^+	Incident voltage
Z_L	Load impedance

CHAPTER ONE

1. Introduction

1.1 Background

Fifth Generation antenna design is currently the most researched subject in communication systems. As predicted, 5G will be accessible in nearly all countries by 2021 [1]. The Fifth Generation technology is anticipated to focus on improving the fourth generation technology, enabling approaches to the 4G shortage such as limited bandwidth and data transfer rate [2].

Since the first generation of mobile network standards arrived in 1982, a new standard generation has developed every 10 years or so. These standards are being created to meet the current and future needs of mobile users. However, global mobile traffic is expanding at an exponential rate each year, and this trend is projected to continue in the near future [3].

Global mobile data traffic will almost definitely continue to increase rapidly in the coming decade. Naturally, there is a rising fear that the current cellular network capacity will not be sustainable in the long run. Several research foundations and business partners have been investigating the concept of a 5th generation (5G) mobile network with improved capacity, latency, and mobility in recent years [4]. Due to a lack of spectrum in conventional microwave bands, millimeter wave (mm-Wave) bands have received a lot of interest as an extra spectrum band for 5G cellular networks [5].

The key concepts of 5G will be aimed at increasing network capacity while providing improved coverage at a reduced cost. The most significant and critical goal of all is "capacity," which is directly related to the increasing customer demand for faster and larger data rates. Massive MIMO is the technology being researched to reach these high data rate requirements. Massive MIMO: Extending the multi-user MIMO idea to hundreds of base station antennas is a possible method for considerably increasing user throughput and network capacity by allowing beam-shaped data transmission and interference management. Higher antenna gains are required to compensate for the greatly increased path loss at very high frequencies, which is made possible

by increasing the number of antennas at the base station. 5G equipment is being researched and developed for sub-1ms latency and lower battery consumption than 4G equipment [6].

Moving to mm-Wave frequencies for 5G mobile stations necessitates new antenna design techniques for mobile-station (MS) and base-station (BS) systems. Smaller antennas stacked in an array can be used to build an effective beam-steerable phased array antenna, which is one of the most critical components for 5G cellular networks [7].

Due to various new applications outside personal communications, the number of devices could reach the tens or even hundreds of billions beyond 5G is achieved [8]. In recent years, the necessity for more spectrum and the demand for high-speed cellular communications have driven the adoption of millimeter wave (mm-wave) carrier frequencies for 5G cellular networks, where high-gain adaptive antennas are used [9]. Because of the tremendous amount of bandwidth available, the mm-Wave spectrum has attracted a lot of attention [5].

The millimeter-wave band is defined as a section of the electromagnetic spectrum spanning from 30 to 300 GHz, with wavelengths ranging from 10 to 1 mm. The recent advancement of silicon technology, as well as the rapidly growing mm-wave application markets (such as automotive radars, high-resolution imaging, and high-definition video transfer requirements), necessitate the development of broadband, highly integrated, low-power, low-cost wireless systems, including high-efficiency planar antennas [10]. Because of their low cost, ease of manufacture, and promise of high-efficiency operation, integrated planar antennas have sparked a lot of interest in mm-wave applications in recent years. The tiny wavelength at mm-wave frequencies helps in the creation of small and efficient antennas. However, at mm-wave frequencies, losses are often larger than at lower frequencies; therefore, the antenna designer must carefully construct the antenna and select a suitable substrate to reduce losses and achieve high radiation efficiency [10].

Because of their short wave length, mm-wave antennas may be made smaller than traditional cellular frequency waves. Because of the compact size of the antenna, it is possible to use sharp beam shaping or massive MIMO technology [11]. Small-sized antennas are in demand in 5G network infrastructure as they are capable of high frequency applications, which, in turn, makes

microstrip patch antennas one of the most effective and convenient antennas available for use [12]. Many types of antennas have been designed to meet the requirements of the 28 GHz band for 5G technology. Several researchers have proposed microstrip patch antennas to operate at 28 GHz using different substrate thicknesses. Moreover, it is noticed that using a thicker substrate with a lower permittivity value increases the antenna's overall efficiency, but it leads to an enlargement of the antenna's dimension. Therefore, it is complex to balance the trade-off between the antenna's size and performance. In fifth generation technology, particularly in wireless communication systems, wide bandwidth and smaller geometry are important, undoubtedly.

The key objective of this thesis is to design and analyze the antenna with slotted ground plane and slotted microstrip patch antennas that are proposed to be improved with bandwidth, compact size, and slotted microstrip patch array antennas that need to achieve high gain for wireless applications. To obtain these objectives, optimizing the slot of the antenna is performed to identify the slot size and slot position, which play a major role in the antenna's reflection coefficient, bandwidth, and resonant frequency. After identification of the slot size and slot position of an antenna, a new slot shape for single-element antennas and antenna arrays is proposed, which performs wide bandwidth, high gain, and high radiation efficiency.

1.2 Motivation

This study included a thorough examination of several aspects that affect antenna performance (such as antenna type, feeding technique, substrate dielectric constant, substrate thickness, substrate loss tangent, and so on). The study's utility is demonstrated by the construction of a slotted MSPA antenna and arrays optimized for wireless communication systems. The proposed antenna is built for the millimeter wave frequency range and has the following design features: The proposed antenna has a wide bandwidth of more than 1 GHz, with a strong impedance matching of $S_{11} < -10$ dB and consistent radiation patterns capable of supporting the expected high data rates of networks. To compensate for the additional path loss at mm-wave frequencies, the proposed design of slotted microstrip patch antenna arrays has high gain and radiation efficiency.

1.3 Statement of Problem

The main limitations of microstrip patch antennas are their narrow bandwidth, low gain, and radiation efficiency, which affect wireless communication applications. The bandwidth of a microstrip antenna can be improved by increasing the height of the substrate by using the transmission line model. At the same time, increasing the height of the substrate also increases the surface waves, which move from end to end around the substrate and spread at the curves of the radiating patch, which adopt the energy of the signal, thus declining the antenna's performance. In order to avoid this problem, different techniques are used, such as the slotted ground plane and the slotted radiated patch technique, to achieve wide bandwidth and higher antenna performance. Further, slotted MSPA plays an important role in the bandwidth of antennas and arrays to increase the gain of antennas. Antennas having the minimum possible size are considered efficient.

1.3 Objectives

1.3.1 General objective

The main aim of this work is to Design and Analysis of Slotted Ground Plane and Slotted Patch Microstrip Array Antenna for Wireless Communications.

1.3.2 Specific objectives

This study is carried out specifically to accomplish the followings:

- To design single element Slotted Ground Plane and Slotted Patch microstrip patch antenna.
- To design (4x1) Slotted Ground Plane and Slotted Patch microstrip patch array antenna.
- A comparison of performance with the single and four by one Slotted Ground Plane and Slotted Patch microstrip antennas design.
- Comparisons of performance proposed antennas with other existing published antenna design.
- To obtain VSWR, Radiation Patterns, return loss, directivity and Gain of Slotted Ground Plane and Slotted Patch microstrip antenna analyze by using antenna design software CST simulation software.

1.4 Significance of the Study

Wireless technologies are now used in space communication, energy harvesting, inventory tracking, and streaming entertainment to billions of people worldwide. Because of its simple geometry, ease of design, compactness, durability, and low production cost, the microstrip antenna is one of the most popular antennas used in wireless communications today. In the last few years, the weight and size of mobile phones have been drastically reduced. Because of the advancement in this trend, the antenna used for mobile handheld devices must be tiny, light-weight, low profile, and have an omni-directional radiation pattern in the horizontal plane. However, there are still issues with the antenna's performance when interacting with the user's head and hand. The movement of the user when using a mobile hand-held device frequently causes changes in gain, radiation pattern, high return loss, and input impedance. As a result, antennas used in personal communication hand-held transceivers have been identified as key elements that can either improve or limit system performance. This is especially true when it comes to bandwidth and efficiency. As a result, in order to properly build a handset with exceptional performance, engineers must pay close attention to the design of the mobile transceiver's antenna systems.

The present wireless communication business is expanding at such a rapid pace that all communication systems are integrating numerous applications such as WLAN, Bluetooth, and so on onto handheld devices. Most wireless protocols will be used in mobile devices in 5G. Antenna isolation is a difficult challenge to tackle due to the near proximity of antennas in space-constrained devices, particularly MIMO devices. Another issue is the limited space available on most mobile devices. To meet this problem, we require designs that have a consistent radiation pattern, are straightforward to integrate with RF circuits, have a low profile, are efficient, and can be polarized throughout a wide frequency band. Another difficult challenge is modeling massive antennas to forecast their performance. One solution is to construct a slotted micro strip patch array antenna to improve antenna gain, directivity, efficiency, bandwidth, and to minimize antenna array mutual coupling.

1.5 Scope and limitations of the study

The goal of this proposed research is to create a suitable slotted ground plane and slotted patch array antenna for 5G applications using antenna design software called Computer Simulation Technology. The antenna perspective is used to describe the wireless communication idea. The steps for creating a single rectangular patch antenna are investigated. To facilitate the development of the basic design of a slotted rectangular patch antenna, a patch parameter was derived analytically, and antenna parameters were optimized using CST software. Based on a single patch antenna, an array slotted ground plane and a slotted patch antenna are constructed. To meet the 5G technology requirements, the antenna must have a wide band width and high gain. CST software is used to examine the antenna's VSWR, Return Loss, Radiation Patterns, Directivity, and Gain for 5G wireless communications.

1.6 Methodology

The methods employing to achieve the objective of this proposed research work are:

- **Literature review:** this includes reading of books, articles, journals and simulation tools and all forms of other resources which are related to slotted microstrip patch antenna.
- **Design specification:** this involves identify of resonate frequency, substrate height, dielectric constant and microstrip patch geometry.
- **MSPA parameters:** this includes determining mathematical calculation of the microstrip patches antenna and feeding line parameters.
- **Simulation:** this is the approximation of the modeling slotted ground plane and slotted patch antenna/array in CST, to investigate performance of the band width, VSWR, Return Loss, directivity and Gain Simulation.
- **Performance comparison:** this involves the antenna gain, directivity, VSWR, Return Loss, Radiation efficiency, and radiation pattern used performance comparison and explanation which is based on the results and findings obtained from the simulated results CST.

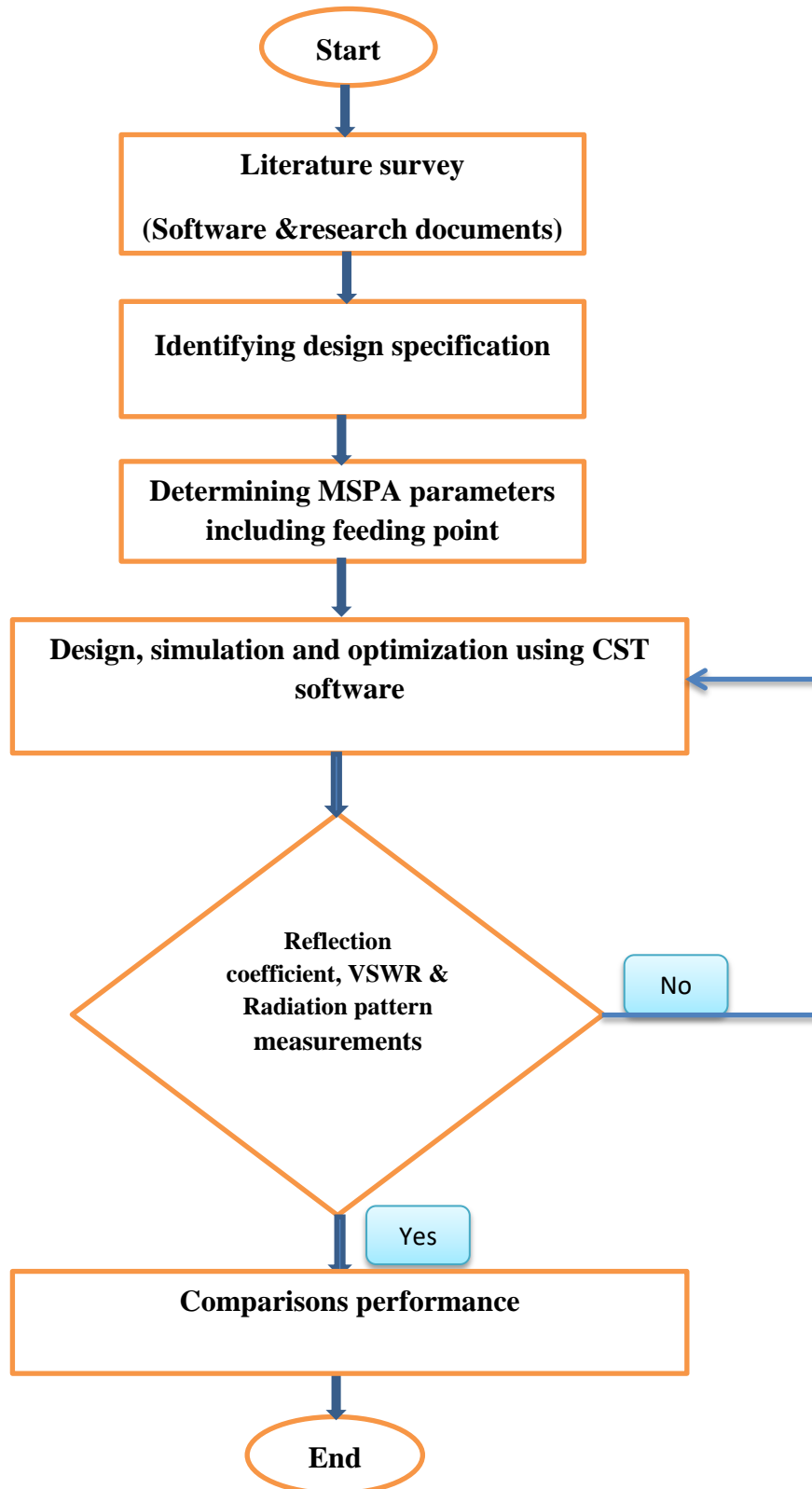


Figure 1. 1: Flow chart of methodology

1.7 Contribution

Varied slotted microstrip patch antenna design and modeling have been examined at different slot shapes and sizes of design parameters in all of the literature seen thus far in the following chapter. The following points are contributions to this thesis study:

- Single element slotted microstrip patch antennas for wireless communication was designed in this thesis. Ultra-wide bandwidth, minimum return loss, and high radiation efficiency have been achieved with the proposed design.
- In this thesis, 4X1 slotted rectangular microstrip patch antenna arrays for wireless communication were designed. This proposed array operates in dual bands, which means higher gain and directivity have been achieved.
- The proposed array antenna operates with dual band capabilities.
- The proposed antenna is small in size.

1.8 Thesis Organization

This thesis work is organized into six chapters. Chapter one is an introductory section. Chapter two talks about antenna theory, antenna parameters, and related work by researchers. In chapter three, microstrip patches and arrays of antennas have been discussed. Chapter four designs slotted rectangular patch antennas and arrays. The fifth chapter is all about simulation and discussing the results. Chapter six concludes with new research ideas for the future.

CHAPTER TWO

2. Literature Review and Antenna Theory

2.1 Introduction to Antenna Theory

An antenna is particularly significant in a radio system since it transmits and receives radio waves. It is intended to convert guided electromagnetic waves in a waveguide, feeder cable, or transmission line into radiating free space waves and, through reciprocity, to gather power from passing electromagnetic waves. As a result, antennas should provide radiation efficiency [6] [32]. Figure 2.1 depicts how an antenna acts as a transition area between directed and propagating waves.

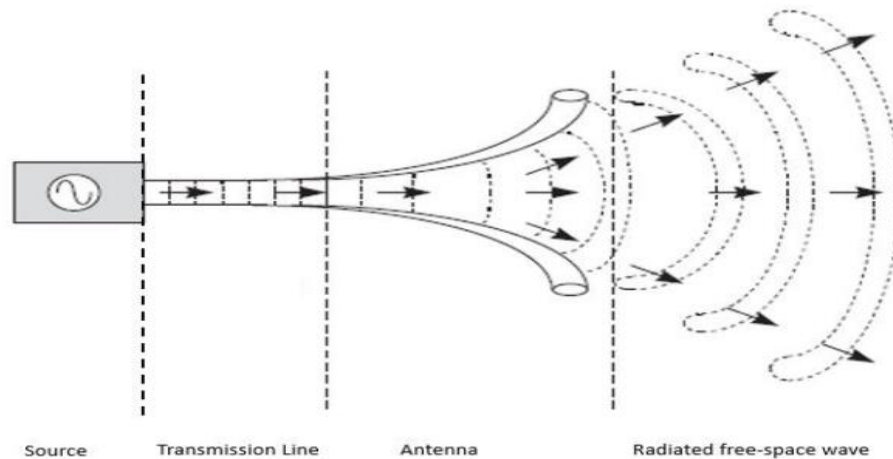


Figure 2. 1: The antenna as a transition region between guided and propagating waves [6]

As shown in Figure 2.2, a transmission-line electrical equivalent circuit can be used to mimic the antenna in transmission line mode. An ideal generator is used to simulate the source, which is coupled to the antenna through an impedance-controlled transmission line. The antenna resistance R_a is represented by two elements: the conduction and dielectric ohmic losses R_o and the radiation resistance R_r , while its reactance X_a represents the imaginary part of the impedance associated with the antenna radiation, which models the energy stored in the antenna near field.

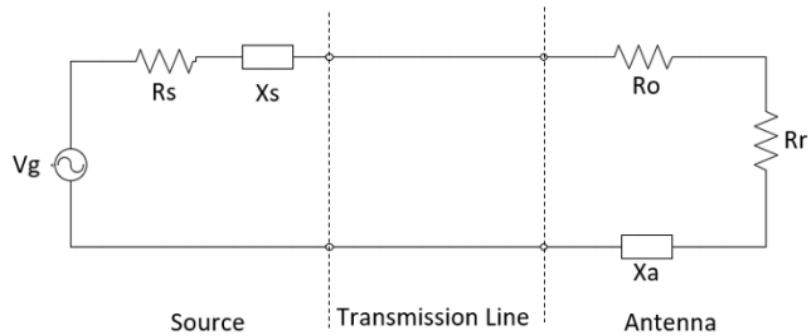


Figure 2. 2: Transmission line equivalent circuit of antenna in transmitting mode [6]

High operational frequency is the first issue for 5G networks. On the other hand, Mm-waves have considerably different propagation circumstances, air absorption, and hardware constraints than centimeter-waves. These difficulties could be mitigated by employing beam shaping and a bigger antenna array. To reduce significant path loss, it is widely agreed that the mm-wave band must be employed with a small cell radius (100 m). When increasing the operating frequency from 2 GHz to 28 GHz or 70 GHz, there will be an additional path loss of approximately 23 and 31 dB, respectively [54].

A second difficulty is signal attenuation in high frequency bands. This is a significant problem since it restricts signal propagation. Because the oxygen molecule absorbs electromagnetic energy at around 60 GHz, the free-licensed band from 57–64 GHz has substantial oxygen absorption with an attenuation of about 15 dB/km. Furthermore, water vapor absorbs electromagnetic radiation with considerably greater attenuation at 164–200 GHz [54].

A third issue is that millimeter-wave transmissions penetrate solid objects with very high losses, making them too sensitive to obstructions like buildings. Due to high levels of attenuation, millimeter-wave communication from outside cells may be limited to only outdoor receivers. Indoor millimeter-wave small cells or Wi-Fi solutions would thus provide coverage.

There is unutilized or underutilized Local Multipoint Distribution Service broadband spectrum at 28 GHz, and given the low atmospheric absorption, the spectrum at 28 GHz has very comparable open space path loss to today's 1-2 GHz cellular bands, as mentioned in [54]. Furthermore, rain attenuation and oxygen loss do not considerably increase at 28 GHz, and in fact, when

considering the availability of high-gain adaptive antennas and cell sizes in the range of 200 meters, 28 GHz may offer better propagation circumstances than today's cellular networks.

2.2 Antenna Fundamentals

The parameters that control the performance of an antenna include: input impedance, VSWR, reflection coefficient, efficiency, gain, bandwidth and radiation patterns. These characteristics are discussed in the following sections.

2.2.1 Input Impedance

It is defined as the ratio of the voltage to the current at the input terminal of an antenna. It is a frequency dependent function. In order to transfer maximum power to an antenna in accordance with the maximum power transfer theorem, the impedance of the transmission line or the coaxial cable must be equal to the conjugate of the input impedance of the antenna as given in Equation 2.1[6]. This is known as proper matching [6]

$$Z_l = Z_a \quad (2.1)$$

Z_l and Z_a are the impedance of the feeding line and the input impedance of the antenna respectively.

2.2.2 Voltage Standing Wave Ratio

It is simply known as VSWR and it can be explained by considering the voltage at different locations of the coaxial cable feeding an antenna. A fraction of the incident power is reflected back in opposite direction towards the transmitter from a mismatched antenna, so at some points along the cable the incident and the reflected waves are in phase and other points the two waves are out of phase, resulting in standing wave pattern. The ratio of the maximum voltage to the minimum voltage at these two locations on the coaxial cable is known as voltage standing wave ratio. VSWR is given by Equations 2.2 [6].

$$VSWR = \frac{V_{max}}{V_{min}} \quad (2.2)$$

2.2.3 Return Loss

The loss of power in the reflected signal due to impedance mismatch is known as return loss and is given by [6]:

$$RL(dB) = 10 \log_{10} \frac{P_i}{P_r} \quad (2.3)$$

Where P_i and P_r are the incident and the reflected powers respectively. The return loss in the above equation is in dB. Its sign is positive and a high return loss is desirable in case of an antenna as it represents a good match. In other words, increase in return loss is due to decrease in the reflection coefficient. However, in literature, it is widely represented by a negative number [6]. Basically the negative of the magnitude of the reflection coefficient in dB is the return loss and it is given by Equation 2.4 [6]

$$RL(dB) = -20 \log_{10} |\Gamma| \quad (2.4)$$

$|\Gamma|$ represents the magnitude of the reflection coefficient in the above equation. The large value of the return loss indicates that the reflected power is small as compared to the incident power and it will be entirely zero if the antenna is perfectly matched to the feeding line.

2.2.4 Antenna Efficiency

There are two types of antenna's efficiencies; (i) radiation efficiency and (ii) total efficiency. The antenna total efficiency is defined as the ratio of the power that is radiated by an antenna to the power delivered to the antenna. The ratio of the power radiated by an antenna to the power input of the antenna is called radiation efficiency. The radiation efficiency e_R is given by Equation 2.5 [6].

$$e_R = \frac{P_{rad}}{P_{input}} \quad (2.5)$$

While the product of the loss of the antenna due to impedance mismatch i.e. M_L and the radiation efficiency is called total efficiency. The total efficiency is given by Equation 2.6 [6]

$$e_T = M_L \times e_R \quad (2.6)$$

Obviously the radiation efficiency is always greater than the total efficiency. The losses in an antenna are the reflection losses that are caused by the mismatch between the transmitter and the antenna, the conduction (I^2R) losses caused by the conductor and dielectric losses due to the dielectric of the antenna [6].

2.2.5 Gain

The gain of an antenna is also calculated with reference to the isotropic radiator. It is defined as the ratio of the radiation intensity of an antenna in the direction of (θ, ϕ) to the radiation intensity of the isotropic radiator if the isotropic radiator is given the same input power as that of the practical antenna. The gain of an antenna is explained with the help of Figure 2.3 [6].

$$G(\theta, \phi) = \frac{U}{U_i} \quad (2.7)$$

The radiation intensity of the isotropic radiator is given by [6]

$$U_i = \frac{P_{in}}{4\pi} \quad (2.8)$$

So finally the gain of the antenna is [6]

$$G(\theta, \phi) = \frac{4\pi U}{P_{in}} \quad (2.9)$$

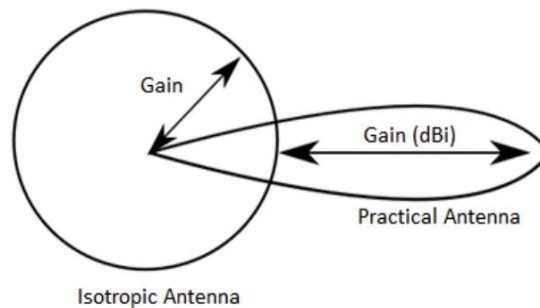


Figure 2. 3: Concept of an Antenna's Gain [47]

The gain of the antenna in decibel (dBi) is given by [6]

$$G_{dB} = 10 \log_{10} G(\theta, \phi) \quad (2.10)$$

The gain of an antenna combines the efficiency and the directivity. Following is the well-known relationship between the gain and the directivity of an antenna [6]

$$G = e_R \times D \quad (2.11)$$

Basically gain is the ability of an antenna to focus its radiations in a particular direction in the far field during transmission and its ability to receive the energy in that particular direction during reception.

2.2.6 Bandwidth

The range of frequencies in which an antenna operates satisfactorily is called the bandwidth of the antenna. Basically it is the difference between the higher frequency f_H and the lower frequency f_L in the given operating spectrum. Mathematically it is defined as [6]

$$BW = f_H - f_L \quad (2.12)$$

The ratio of the bandwidth to the center resonant frequency is known as fractional bandwidth. The percentage fractional bandwidth is represented by FBW [6].

$$FBW = \frac{BW}{f_c} \times 100 \quad (2.13)$$

f_c in the preceding equation is the center resonant frequency of the bandwidth. The bandwidth of the MSPA is governed by the impedance bandwidth. In the impedance bandwidth the reflection coefficient of the MSPA is less than -10dB.

2.2.7 Radiation Pattern

The energy radiated by an antenna in space is represented by its radiation pattern. The graphical representation of the far field radiation of an antenna as a function of spherical coordinates θ and ϕ at a constant radial distance r is known as the radiation pattern [6]. The 3-dimensional radiation pattern is shown in Figure 2.4. It is represented in spherical coordinates (r, θ, ϕ) with the assumption that the antenna is at the center of the spherical coordinate system.

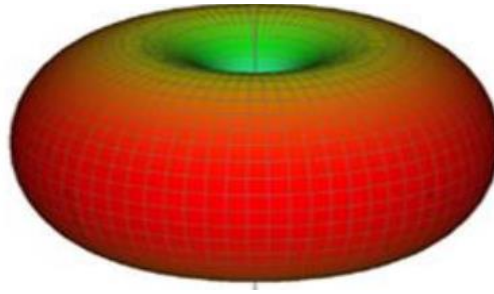


Figure 2. 4: 3D Radiation Pattern [48]

For 2-D radiation pattern, the x-y plane ($\theta = 90$) is the azimuth or horizontal plane.

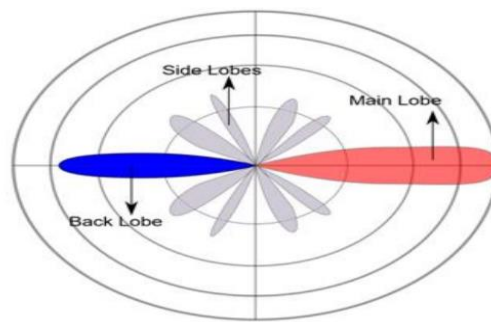


Figure 2. 5: 2D radiation Pattern [49]

The y-z plane at ($\phi = 90$) that is normal to the horizontal (azimuth) plane is the elevation or vertical plane. The 2-D radiation pattern has three lobes, main lobe, side lobe and the back lobe as shown in Figure 2.5[6]. Most of the energy of the antenna exists in the main lobe. The angle between the half-power points of the main lobe with respect to the maximum radiated power defines the half power beamwidth of the radiation pattern. It is represented by HPBW as shown in Figure 2.6 [6]

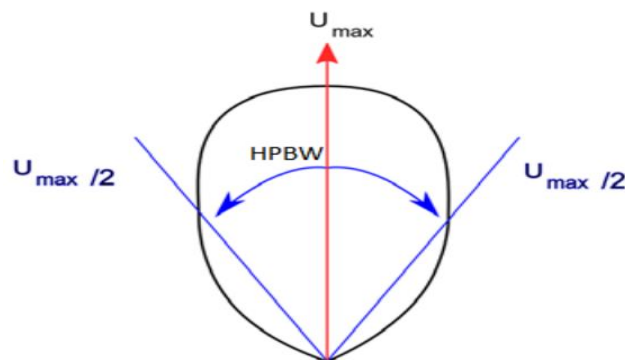


Figure 2. 6: Half Power Beamwidth [50]

2.3 Related Work

The relevant research literature for the enhancement of the different characteristics of the patch antennas is illustrated in the following sections. The creation of slots on the patch of the antenna improves the impedance matching, especially at higher frequencies. It changes the distribution of current, due to which the current path length and the input impedance of the patch antenna changes. The addition of slots to the patch of the antenna results in a new resonance frequency, thus two or more resonance regions are created, which enhances bandwidth [13]. Different shapes of patches like U-shape, E-shape, M-shape and A-shape have been designed in [14-17] for the improvement of the impedance bandwidth of MSPA. According to [18] the substrate material plays significant role determining the size and bandwidth of an antenna. Increasing the dielectric constant decreases the size but lowers the bandwidth and efficiency of the antenna while decreasing the dielectric constant increases the bandwidth but with an increase in size.

Some problems related to MSPA have been addressed with the use of creation of slots on the ground plane[19]. Slots on the ground plane includes advantages such as decrease in the patch size and enhancement in gain and bandwidth [20]. A G-shaped slot on ground plane has been explained in [21] and it has been claimed that the slot had improved both the return loss and the impedance bandwidth. A compact patch antenna of size $17 \times 17 \times 1.07 \text{ mm}^3$ with slot on the patch and DGS has been investigated in [22] and it has been concluded that the proposed antenna on FR-4 substrate had a bandwidth of 1.23GHz. The height of the substrate is 1 and its dielectric constant is 4.9. Two rectangular slots on the patch and rectangular DGS have been presented in this work.

In [23] this paper aim is to design the MIMO 8×8 MSPA with 2 H-slot rectangular patches array with 5G radio access system at frequency range 14.5 to 15.25 GHz. However, dealing with MIMO, there will be great challenge that is mutual coupling here it is affecting the antenna performance. A compact antenna array design utilizing the concept of connected antenna arrays has been discussed in [24]. CAA presents wideband antenna responses that can be very suitable to mm-wave applications as well as provides more compact antenna sizes that can be integrated within mobile terminals compared to conventional ones. A $100 \times 60 \times 0.76 \text{ mm}^3$ slot-based CAA has been proposed for standard mobile handset size terminals that includes 4G (1.8-

3.1 GHz) and 5G mm-wave (27.2- 28.5 GHz) antenna systems. The reported gain for 5G antennas is about 10 dBi. In [25], a 28GHz 4x4 antenna array has been fabricated for 5G base station applications, with capability to be connected to a RF front-end allowing beamforming. The dimensions of the design are 78.5x42 mm² with 1.5 GHz operating bandwidth and a reported achievable gain of 18 dBi.

In [26], a millimeter-wave flexible antenna for 5G wireless applications is reported. The antenna geometry comprises of a T-shaped patch integrated with symmetrically designed slot arrangements. The measurements of the inkjet-printed antenna prototype depict an impedance bandwidth of 26–40 GHz, consistent omnidirectional radiation pattern, and a peak gain of 7.44 dBi at 39 GHz.

In [27], a novel capacitive coupled patch antenna array design was positioned in the mobile phone chassis as a set of 4 sub-arrays each with 12 antenna elements to provide high gain around 27 dBi with each sub-array providing 90 degree coverage. The antenna array covers the frequency range of 24-28 GHz, a promising band for future 5G based smartphone services. The antenna has 12 radiation elements of 3.7x3.25 mm each with a separation between the 12 elements of 6.3mm.

In [28], a novel mm-wave phased array antenna for whole metal covered 5G mobile handset has been proposed. It consists of eight rotated slot antenna elements arranged on the upper frame of the metal-body. The proposed antenna operates between 27.1 and 28.6 GHz and has hemispherical beam coverage suitable for 5G mobile communication. The 138x67.1x7.1mm³ antenna was configured on the metal body of the handset top section with a gain up to 13.7dBi.

In [29], a 12x28.2x0.4mm³ compact, flexible and wideband mm-wave Franklin antenna array was designed for upcoming 5G applications. Measurements showed that the designed array covers the band 24.6–30 GHz with a simulated gain of 8.3dBi at 28 GHz.

In [30], a novel modified compact broadband antipodal Vivaldi antenna array for future 5G communication systems has been discussed. The proposed structure of 28.823x60x0.787mm³ consists of 8 antenna elements that are fed by a 1-to-8 power divider. Multiple notch structures were added on the ground plane. Impedance bandwidth was extended slightly from 24.65–28.5

GHz to 24.55–28.5 GHz, and the gain improved simultaneously. Measurement results showed a gain of 6.96–11.32 dB in the operating frequency band.

In [31], the design of an 8-element microstrip patch antenna array for dual-band 5G communications is discussed. The proposed antenna array is compact of size $16 \times 16 \text{ mm}^2$. The dual-band responses at 28 and 38 GHz have been achieved by etching an inverted U-shaped slot from the main radiator. Coupling between elements was about -10dB at 28G and -5.5dB at 39.95GHz, with a narrow bandwidth at each resonant frequency range.

In the above literature, all those methods are proposed to enhance the gain and bandwidth of MSPA. The proposed methods have advantage as well disadvantages. Some methods have small bandwidth, low gain and low radiation efficiency. For the proposed antenna, all the advantages are collected and summarized to design a new slotted ground plane and slotted microstrip patch antenna arrays for wireless communications.

CHAPTER THREE

3. Micro strip Patches Antenna

3.1 Introduction

Because it is simple to design and construct, micro strip patches antennas are utilized in a wide range of applications. The antenna is appealing due to its low-profile conformal design, low cost, and extremely narrow bandwidth. Low profile antennas are required for applications where size, weight, cost, performance, ease of installation, and aerodynamics are constraints. Demands for aircraft, spacecraft, satellites, and missiles, as well as mobile radio and wireless communications, have recently increased [1]. Micro strip antennas can be utilized to achieve these needs. These antennas have a low profile, are suitable for planar and non-planar surfaces, are simple and inexpensive to manufacture, are mechanically robust when mounted on rigid surfaces, are compatible with MMIC designs, and are very versatile in terms of resonant frequency, polarization, pattern, and impedance [1]. Furthermore, by inserting loads such as pins and reactor diodes between the patch and the ground plane, adaptive elements with changeable resonant frequency, impedance, polarization, and pattern can be created. In its most basic form, a micro strip antenna consists of a radiating patch on one side of a dielectric substrate with a ground plane on the other, as shown in Figure (3.1). The patch is often constructed of conductive material such as copper or gold and can take any shape. Typically, the radiating patch and feed lines is photo etched on the dielectric substrate.

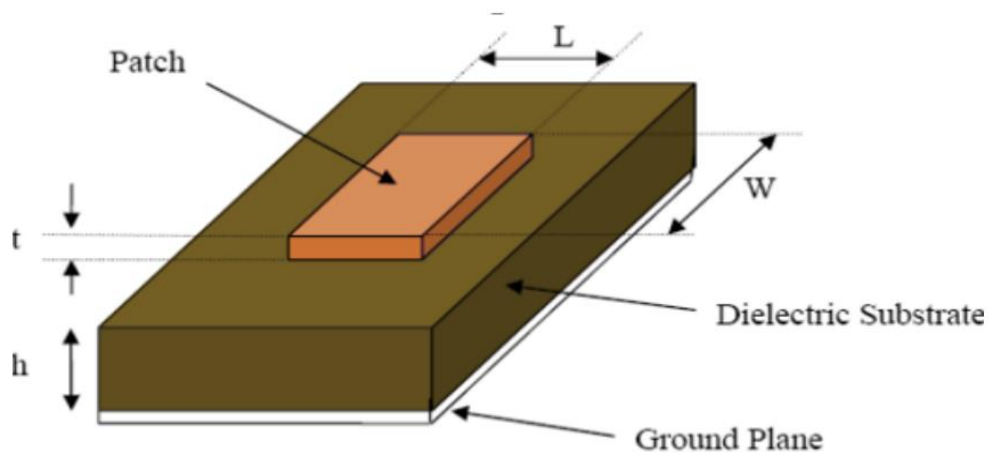


Figure 3. 1: Rectangular Patch Antenna [6]

In order to simplify the analysis and performance prediction, the patch is generally square, rectangular, circular, triangular, and elliptical or some other common shape as shown in Figure 3.2 below. For a rectangular patch, the length L of the patch is usually $0.3333\lambda_0 \leq L \leq 0.5\lambda_0$, where λ_0 is the wavelength of free space. The patch is selected to be very thin such that $t \leq \lambda_0$, where t is the thickness of patch. The height of dielectric substrate is usually $0.003\lambda_0 \leq h \leq 0.5\lambda_0$. The dielectric constant of the substrate (ϵ_r) is typically in the range $2.2 \leq \epsilon_r \leq 12$ [62].

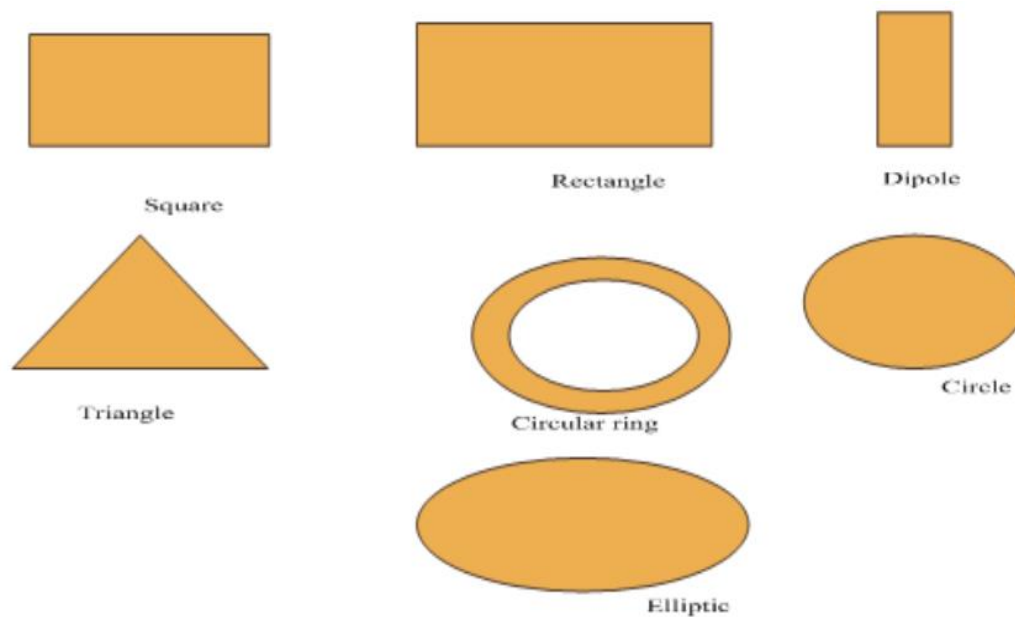


Figure 3. 2: Common Available Shape of Micro strip Antenna [21]

The fringing fields between the patch edge and the ground plane are principally responsible for the radiation of micro strip patch antennas. A thick dielectric substrate with a low dielectric constant is preferable for superior antenna performance because it gives better efficiency, a narrower bandwidth, and better radiation. However, this configuration results in a bigger antenna size. In order to create a compact Micro strip patch antenna, substrates with higher dielectric constants must be employed, which results in a bigger bandwidth and reduced efficiency. As a result, a trade-off must be made between antenna size and antenna performance. Arrays of micro strip elements with single or multiple feeds can also be employed to provide scanning capabilities and attain higher directives.

3.2 Advantages and Disadvantages of MSPA

The microstrip patch antennas have made a great progress in the last few decades as they have enormous advantages as compared to traditional antennas. These antennas have advantages like the low profile, small dimensions, low volume, very light weight, economical, conformable to the planer and non-planer surfaces and easy to fabricate. They occupy a very small volume during installation. They are manufactured very inexpensively and easily using modern printed circuit technology. However, a few major disadvantages of these microstrip patch antennas include low gain, very low impedance bandwidth and low efficiency.

3.3 Antenna Feeding Techniques

A microstrip patch antenna is excited with a number of techniques as explained in the following sections [6]. The microstrip line feed, coaxial probe feed, aperture coupling and coupled indirect feed have been explained in the upcoming sections.

3.3.1 Probe feed

This is a very common method to excite a patch antenna. The inner conductor of the coaxial cable is connected to the patch while the outer conductor is connected to the ground plane as shown in Figure 1.4[66]. The advantages of the coaxial cable are that the cable can be placed at a desirable location for appropriate matching and can be fabricated easily.

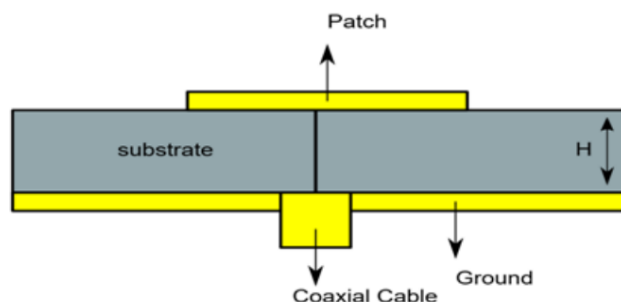


Figure 3. 3: Coaxial Probe Feed [66]

3.3.2 Microstrip feeds

A microstrip feed can be fabricated on the same plane as the patch antenna. It is easy to match by controlling the inset position and easy to model in the design simulations. It can be designed as an inset feed, a quart-wavelength transmission line feed, or a microstrip line feed. However, the

disadvantage of this method is that as substrate thickness increases, surface wave and spurious feed radiation also increase, which limits the bandwidth. A patch antenna is excited with the help of a microstrip transmission line, as shown in Figure 1.3a. The width of the conducting strip is small as compared to the patch's width. The microstrip transmission line is etched on the same planar surface of the substrate and is connected to the patch [62]. The parameter L represents the length of the patch, and the width of the patch is represented by W . The microstrip line feeding technique that is shown in Figure 3.4 is also known as Inset Feed.

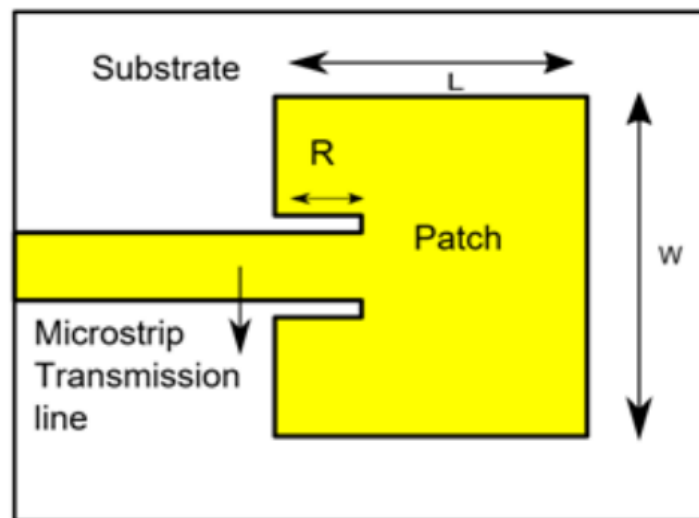


Figure 3. 4: 2D View of Microstrip Transmission Line Feed [62]

3.3.3 Aperture coupling feed

The aperture coupling feed technology is a newer non-contact feeding method. It is made up of two substrates that are separated by a ground plane. A microstrip feed line on the bottom side of the lower substrate couples energy to the patch via a slot in the ground plane Figure 3.5. This arrangement enables the feed mechanism and the radiating element substrate to be optimized independently. For the bottom substrate, a high dielectric material is utilized to produce tightly linked fields that do not cause spurious radiation, while a thick low dielectric constant material is used for the top substrate to produce generally wide fringing fields that produce better radiation. The ground plane between the substrates additionally isolates the feed from the radiating element and reduces spurious radiation interferences for pattern and polarization purity. However, this feeding strategy will increase the overall thickness of the design, which is undesirable for space-

constrained mobile devices. It also makes fabrication more complicated, which is not ideal for commercial mass production [6].

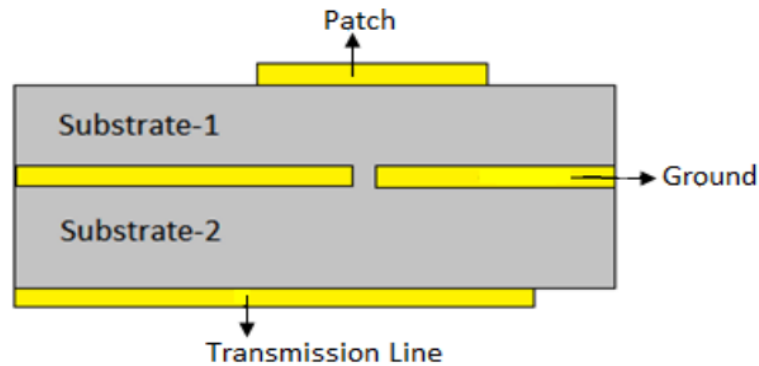


Figure 3. 5: Aperture Coupling [62]

3.3.4 Coupled Indirect Feed

This kind of feeding mechanism does not touch the patch directly as shown in Figure 3.6[63].The gap between the patch and the feed line introduces a capacitance that cancels out the inductance of the feed line. The antenna is excited with the help of Microstrip transmission line.

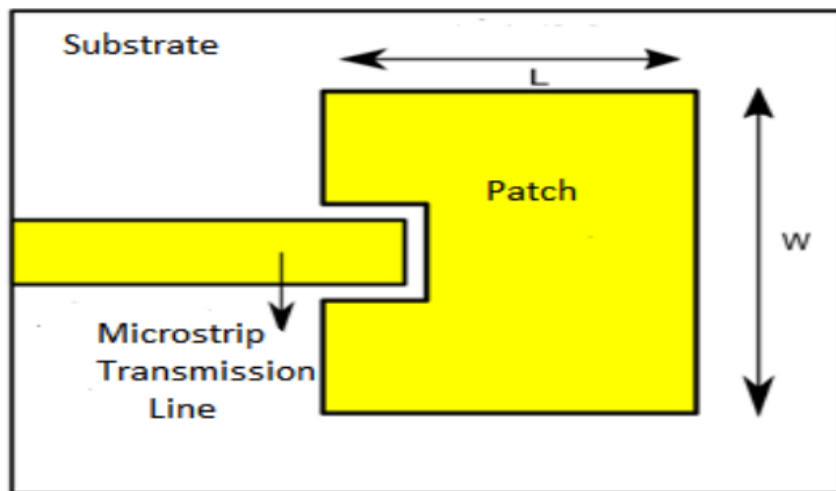


Figure 3. 6: Coupled Indirect Feed [62]

3.4 Micro strips Array

The antenna must have a high gain of more than 12 dB and a direct beam that can be guided in a specific direction for 5G applications [58]. It may be difficult to attain such a high gain with a single tiny antenna. Several small antennas, however, can be put together in an antenna array to

generate such a high-gain directional pattern that can be electronically scanned in a certain direction. The amplitude and phase of the currents feeding individual elements of the array can be adjusted to shape the array radiation pattern by adjusting the element to element separation and the excitation adjustment of the magnitude and phase of the currents feeding individual elements of the array. The array elements can be distributed spatially to form a linear, planar, or volume array. Linear arrays feature a narrow radiation beam in the plane of the array axis and a large beam in the orthogonal plane. This feature of linear array patterns is useful in 5G handset applications because it only takes 1-D scanning to cover a large region. This section begins with a quick examination of the antenna array factor. Following that, a study of mutual interaction between nearby elements and feeding strategies is described.

The following are the primary parameters that influence an antenna array's overall performance [67]:

- Distance between adjacent elements.
- Geometry (e.g., linear, circular, or planar arrangement of the radiating elements).
- Amplitude current excitation of each individual element.
- Phase excitation of each individual element.
- Radiation pattern of each individual element.

3.4.1 The Array Factor for Linear Arrays

The linear array is the most basic design for array elements, as seen in Figure (3.8), where the variable resistance symbol represents attenuators and the other symbol represents phase shifters. Because antennas usually satisfy the criteria of reciprocity, the pattern characteristics of an array may be explained for functioning as a transmitter or receiver. The attenuators and phase shifters can modify the amplitude and phase of each element's output. Amplitude and phase control allow for specific sculpting of the radiation pattern as well as scanning in space [56].

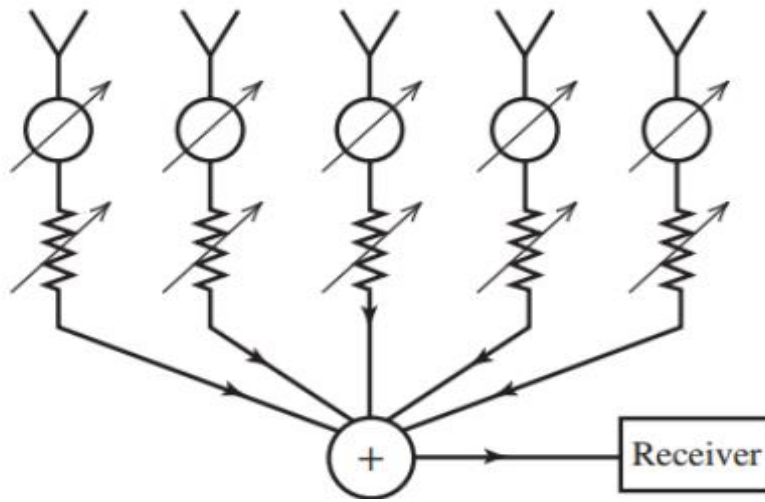


Figure 3. 7:A typical linear array [56].

By replacing each element by an isotropic radiator, the array factor corresponding to the linear array of Figure (3.8) can be found, while maintaining the element locations and excitations, the array is receiving a plane wave arriving at an angle θ from the line of the elements as shown in Figure (3.9), and all the planes with equal phase. Each element is excited with phase ξ_n due to the spatial phase delay effect of the incoming plane wave. The amplitudes of excitation are constant, taken to be unity, because a plane wave has uniform amplitude, as shown in Figure (3.9). The resulting excitations of $Ie^{j\xi_0}$, $Ie^{j\xi_1}$, for each element, then The array factor for this receiving array as in Figure (3.9), is then the sum of the isotropic radiator receiving antenna responses $\{ 1e^{j\xi_0}, 1e^{j\xi_1}, \dots \}$ weighted by the amplitude and phase shift appeared by complex currents $\{ I_0, I_1, \dots \}$ introduced in the transmission path connected to each element. The array factor of the array is thus [56]:

$$AF = I_0 e^{j\xi_0} + I_1 e^{j\xi_1} + I_2 e^{j\xi_2} + \dots \quad (3.3)$$

Where ξ_0, ξ_1, \dots are the phases of an incoming plane wave at the element locations.

The formula equation (3.3) is general for any geometry. Now we consider linear arrays with elements equally spaced along the z-axis as illustrated in Figure 3.8. The phase of the arriving plane wave is set to zero at the origin for suitability, thus $\xi_0 = 0$. The received waves arriving at Element 1 lag the received waves arriving at the origin by a distance of $d \cos \theta$. The

corresponding phase of waves at Element 1 relative to the origin is $\xi_1 = d\cos\theta$ the spatial phase delay. Using this result in equation (3.3) gives [59]

$$AF = I_0 + I_1 e^{j\beta_1 d \cos\theta} + I_2 e^{j\beta_2 d \cos\theta} + \dots + I_n e^{j\beta_n d \cos\theta} = \sum I_n e^{j\beta_n d \cos\theta} \quad (3.4)$$

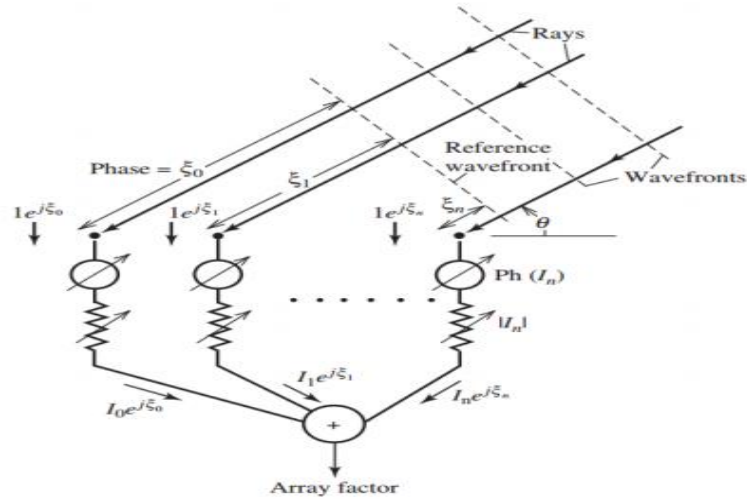


Figure 3. 8: Equivalent configuration of the array[56]

Now the array considered to be transmitting. If the current has a linear phase head way [55]

$$I_n = A_n e^{jn\theta} \quad (3.5)$$

relative phase between adjacent elements is the same), the phase can be separated explicitly as Where the $n+1^{\text{th}}$ element leads the n^{th} element in phase by α . Then Figure 3.10 become [55]

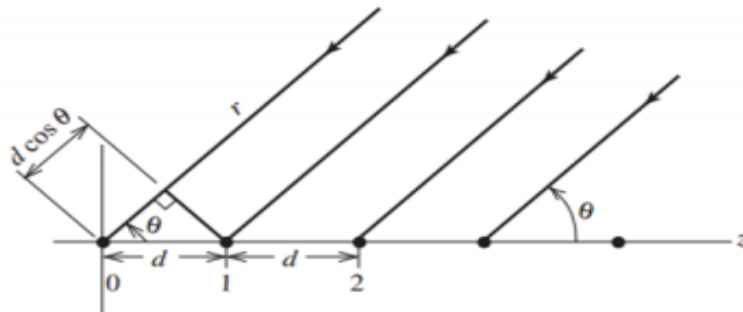


Figure 3. 9: Equally spaced linear array of isotropic point sources [56].

$$AF = \sum_{N=0}^{N-1} A_0 e^{jn(\beta d \cos\theta + \alpha)} \quad (3.6)$$

Define [6]

$$\varphi = \beta d \cos \theta + \alpha \quad (3.7)$$

Then

$$AF = \sum_{n=0}^{N-1} A_0 e^{jn\varphi} \quad (3.8)$$

Generally, the far-field pattern of an array is given by the multiplication pattern of the single element and the array factor, as in Figure (3.11) [6].

$$\text{Total Pattern} = \text{Element Factor} \times \text{Array Factor} \quad (3.9)$$

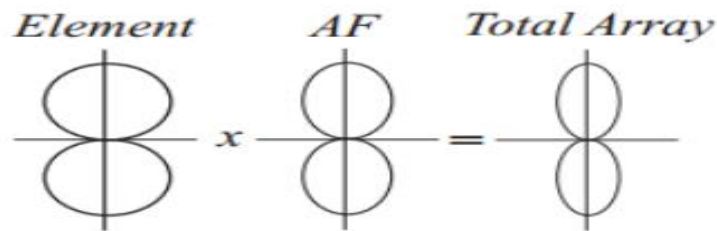


Figure 3. 10: Array radiation pattern [55]

3.5 Antenna Array feeding Configuration

The proper configuration selection depends on many factors, such as bandwidth, the required antenna gain, insertion loss, beam angle, grating/side lobe level, power-handling capability, and polarization.

3.5.1 Parallel Feed

The basic configuration of a one-dimensional parallel feed consists of a branching network of two-way power dividers. Figure 3.11 a corporate feed is the most commonly used parallel feed configuration. The main advantages of parallel feed are that the power is equally split at each junction, the beam position is independent of frequency provided that the distances from the input port to each radiating element are identical, and finally, the feed is broadband [59]. The

bandwidth of a parallel-fed microstrip array is limited by two factors: the patch element's bandwidth and the impedance matching. Depending on the design, a series-fed array can obtain a bandwidth of 1% or less, while a parallel-fed array can achieve a bandwidth of 15% or more [6]. The beam direction can be adjusted by inserting suitable line extensions. The downside of parallel feed is that it necessitates long transmission lines between the input port and the radiating elements, resulting in high insertion loss and lowering the overall efficiency of the array [59]. All radiating elements in the design are typically equally matched to the feed lines using a suitable technology such as a quarter-wave transformer. The number of radiating elements required to create a symmetrical corporate feed network is $2n$, where n is an integer. The parallel-fed array has the relative ease with which both amplitude and phase for each element can be designed independently, while in a series-fed array, one element's change will generally impact all other elements [6].

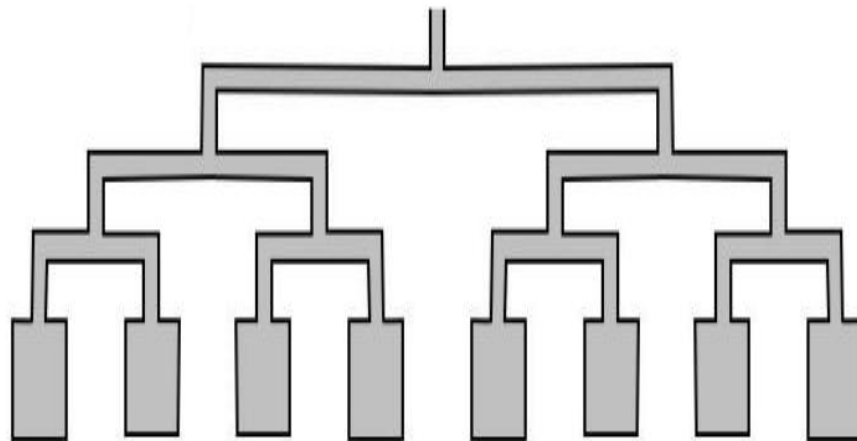


Figure 3. 11: Configurations of parallel feed microstrip array [6].

3.5.2 Series Feed

As shown in Figure 3.12, several elements are organized linearly and fed serially by a single transmission line consisting of a series feed configuration. The Series feed has the lowest insertion loss but generally has the least polarization control and the narrowest bandwidth. It has the narrowest bandwidth since the line passes through the patches, and so the phase between consecutive components is determined not only by line length but also by the input impedances of the patches. Because the patches are amplitude weighted with varying input impedances, the

phases will differ for different elements and will change more dramatically when frequency varies due to the patches' narrowband characteristic [6].

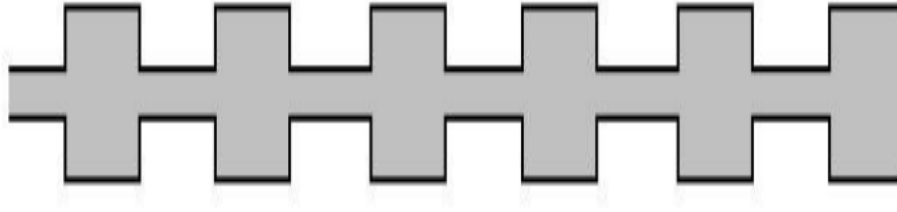


Figure 3. 12: Configurations of series feed microstrip array

3.6 Mutual coupling

3.6.1 Introduction

When designing linear antenna array for 5G we aim to have the largest scanning angle without having grating lobes. This can be achieved by keeping inter-element spacing less than half-wavelength according to (4.8) [56]

$$d < \frac{\lambda}{1+|\cos \theta_0|} \quad (3.10)$$

Where:

λ : Wavelength in free space

d : Inter element space, from center to center

θ_0 : is the main beam pointing angle with respect to the line of the array corresponding to the largest scan angle off broadside.

The goal here is to obtain 180° scanning angle, this can be achieved when $\theta_0 = 0$ and $\cos 0 = 1$ which results in $d < 0.5 \lambda$. This small distance between adjacent elements can cause an increase in the undesired mutual coupling. This affects the current distribution and hence the input impedance as well as the radiation pattern of individual elements. The most significant effects are on the antenna input impedance, which is a very important parameter for a single antenna as well as for an antenna array [55]. A smaller spacing is more desirable for a compact

array because it helps to suppress the grating lobes when scanning. On the other hand, a smaller spacing results in higher coupling.

3.6.2 Mutual Coupling in Antenna Array

The mutual coupling between two radiating elements depends upon the distance between them. If they are close to each other the mutual coupling will be greater. Thus energy is transferred between elements and this is called mutual coupling. One can say that the electromagnetic coupling between the elements is mutual [55].

3.6.3 Reduction of Mutual Coupling

Owing to the recent move toward millimeter wave bands and the massive improvement in manufacturing technologies, the demand for size reduction in the modern communication industry has become a hot topic. However, undesirable mutual coupling (MC) effects arise. It is detrimental to antenna operations through changing the array radiation pattern and the matching impedance of the radiating elements. Moreover, in phased antenna arrays, strong electromagnetic (EM) interactions between radiating elements yield scan blindness and efficiency degradation [64]. Different methods have been used to enhance the isolation between antenna array elements and electromagnetic band gap (EBG) in the substrate as in, using waveguide metamaterials as in, and resonators, such as the I-shaped resonator as in [64].

DGS is able to provide a wide band-stop characteristic in some frequency bands with only one or a small number of unit cells. Due to their excellent pass and rejection frequency band characteristics and their ease of design and fabrication, DGS circuits are widely used in various active and passive microwave and millimeter-wave devices such as filters, dividers, couplers, amplifiers, resonators, and antennas. This defect disturbs the shield current distribution in the ground plane and changes the characteristics of a transmission line such as line capacitance and inductance [65].

CHAPTER FOUR

4. Design of Single Element and 4x1 Slotted MSPA

4.1 Introduction

The basic objective behind this work is to design and analyze slotted microstrip patch antennas having a wide bandwidth, lower return loss, small VSWR, and higher radiation efficiency. This antenna can be used for wireless applications. Initially, a basic rectangular patch antenna has been designed, and then changes have been made to this initial design in light of the literature survey. Thus, a number of antennas have been designed for the improvement of the different characteristics of the patch antenna. The ground plane and the patches of all these antennas are made of pure lossy copper.

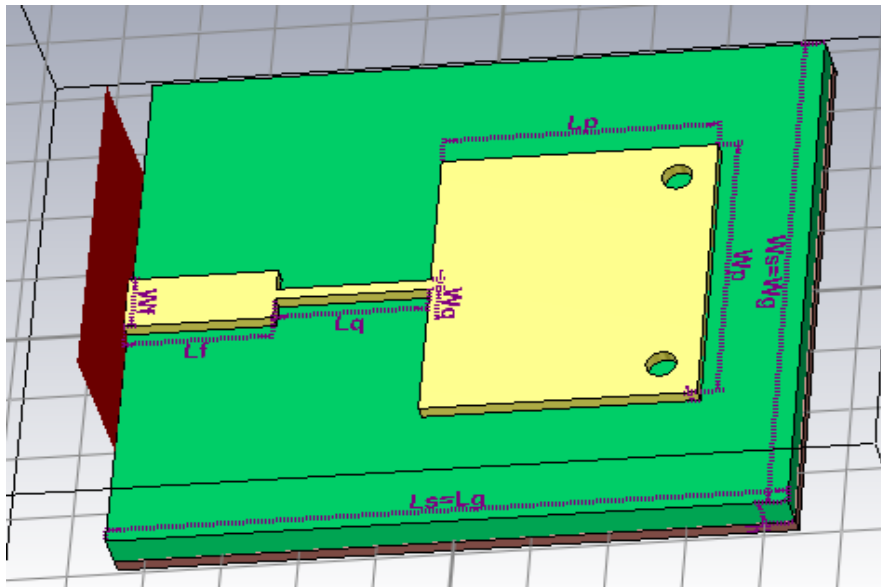


Figure 4. 1: Rectangular Microstrip patch antenna

As shown in Figure 4.1 above, MSPA mainly consists of a ground plane, a radiating patch, and a substrate, where the substrate is used to connect the antenna patch and the ground plane.

4.2 Design Specifications

Before designing the antenna, the first step is to consider the specifications of the antenna based on its application. In this study, the rectangular patch shape was selected because it has wide bandwidth by reason of its broader shape as compared to other types. The various parameters

that are used for the thesis are taken from the data sheet of Roger RT/Duriod and listed in Table 4.1. The frequency range of 24GHz-52GHz was chosen because the frequency is widely used in high band wireless communications. As for the substrate selection, the major considerations will be the dielectric constant and loss tangent. A high dielectric constant will result in a smaller patch size, but this will generally reduce bandwidth efficiency, and a high loss tangent will reduce the antenna efficiency.

Table 4. 1: Single Patch Antenna Design Specifications.

Parameters	Specification
Type of Antenna	Rectangular patch antenna
Frequency Range	24GHz – 52 GHz
Substrate	Roger RT/Duriod 5880
Dielectric constant	2.2
Loss tangent	0.0009
Substrate height	0.254mm
Conductor thickness	0.008 mm

4.3 Design Equations of MSPA

For the proposed antenna design, an initially rectangular patch is designed with a feed at the bottom of it. For better performance, the impedance match between the patch and the feed has to be maintained. For perfect matching, a quarter-wave transformer is designed in between the patch and the feed. The design equations for a rectangular patch, a microstrip feed line, and a quarter wave transformer are discussed briefly in the following sections.

4.3.1 Patch dimensions Calculations (Wp and Lp)

The micro strip patch antenna calculation of width (W_p), length, the improve length (L_p), and fringe factor L. The width of a rectangular micro strip patch is from equation (4.1) [1]:

$$W_p = \frac{c}{2f_r \sqrt{\frac{\epsilon_r + 1}{2}}} \quad (4.1)$$

The effective dielectric constant of a rectangular micro strip patch is from equation (4.2) [1]:

$$\epsilon_{\text{reff}} = \frac{\epsilon r + 1}{2} + \frac{\epsilon r - 1}{2} \left(1 + 12 \frac{h}{W_p} \right)^{-1/2} \quad (4.2)$$

The length extension of rectangular micro strip patch is equation (4.3) [1]:

$$\Delta L = 0.412h \frac{(\epsilon_{\text{reff}} + 0.3) \left(\frac{W}{h} + 0.264 \right)}{(\epsilon_{\text{reff}} - 0.258) \left(\frac{W}{h} + 0.8 \right)} \quad (4.3)$$

The length of a rectangular micro strip patch is from equation (4.4) [1]:

$$L_p = \frac{c}{2f_r \sqrt{\epsilon_{\text{reff}}}} - 2 \Delta L \quad (4.4)$$

4.3.2 Ground plane dimensions calculation (L_g and W_g)

For infinite ground planes, most of the model is applicable, but for practical considerations, a finite ground plane is required. Same results for finite and infinite ground planes are obtained if, in the case of an infinite ground plane, the size of the ground plane around the periphery is greater than the patch dimensions by six times the thickness of the substrate. Hence, for the proposed design, the dimensions of the ground plane would be given as: [1]

$$L_g = L_p + 6h \quad (4.5)$$

$$W_g = W_p + 6h \quad (4.6)$$

4.3.3 The Feed line calculation

The feed line will be fed to the patch through a matching network, which is a quarter-wave transformer. The impedance of the quarter-wave transformer is given by the equations (4.7–4.10):[6]

$$Z_a = \frac{90 \epsilon_r^2}{\epsilon_{r-1}} \left(\frac{L_p}{W_p} \right)^2 \quad (4.7)$$

Where Z_a = patch impedance [6]

$$Z_{qw} = \sqrt{50 \times Z_a} \quad (4.8)$$

Width of quarter wave transformer can be calculated by putting the value Z_{qw} in equation (4.8) and solving it for W_{qw}

$$Z_{qw} = \frac{60}{\sqrt{\epsilon_r}} \ln \left(\frac{8h}{W_{qw}} + \frac{W_{qw}}{4h} \right) \quad (4.9)$$

Length L_{qw} quarter wave transformer equation (4.10) [6]:-

$$L_{qw} = \frac{\lambda_g}{4\sqrt{\epsilon_{reff}}} \quad (4.10)$$

Width of 50Ω microstrip feed can be found equation (4.11) [21]:-

$$Z_0 = \frac{120\pi}{\sqrt{\epsilon_{reff}} \left(1.393 + \frac{W_f}{h} + \frac{2}{3} \ln \left(\frac{W_f}{h} + 1.444 \right) \right)} \quad (4.11)$$

Length L_f transmission feed line in equation (4.12) [21]:-

$$L_f = \frac{\lambda_0}{4\sqrt{\epsilon_r}} \quad (4.12)$$

4.3.4 Array Calculation

The array antenna consists of a branching network of two-way power dividers. . Figure 4.2 shows the impedance for individual lines in the four element array antenna. The array calculation consists of two parts. The first is the patch calculation and the second is for transmission lines. In this thesis, the corporate feed network is chosen for designing four element array networks.

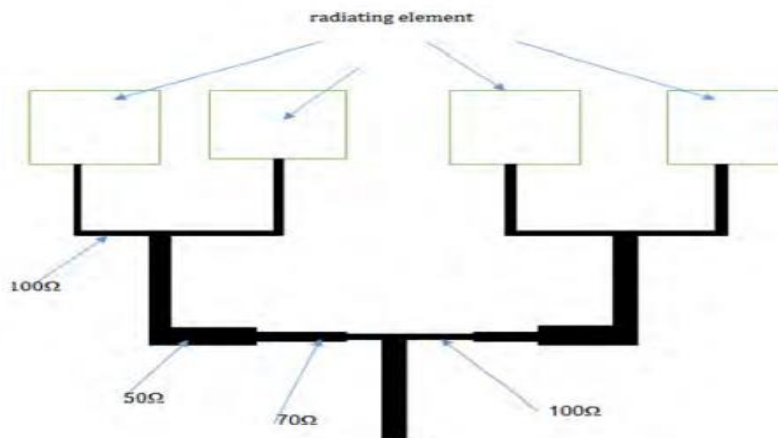


Figure 4. 2: Four Elements Array Line Impedance Design Layout

4.3.5 Calculation of the Impedance for Quarter-Wave Transformer

Using the following equation where by replacing $Z_0 = 50\Omega$ and $R_{in} = 100\Omega$ the transformer Characteristic impedance as illustrate in equation (4.4) [6]:

$$Z_1 = \sqrt{R_{in}Z_0} \quad (4.13)$$

$$Z_1 = \sqrt{100\Omega * 50\Omega} = 70\Omega \quad (4.14)$$

50Ω, 70Ω and 100Ω Transmission Line Calculation As a single patch, the different impedance dimensions are obtained by using the same TX line Calculator.

Therefore, by substituting the initial design parameters in the equations, the remaining physical dimensions of the proposed rectangular MSPA given in Fig 4.2 can be calculated as follows. The antenna parameters are calculated by substituting $C = 3 * 10^8$ m/sec, $h = 0.254$ mm, $\epsilon_r = 2.2$, and $f_0 = 28$ GHz in the equations. (4.1) -(4.12) The dimension of MSPA is:

$$W_p = \frac{C}{2f_r \sqrt{\frac{\epsilon_r + 1}{2}}} = \frac{3 * 10^8 \text{ m/s}}{2 * 28 * 10^9 \text{ Hz} \sqrt{\frac{2.2 + 1}{2}}} = 4.235 \text{ mm}$$

$$\epsilon_{\text{reff}} = \frac{\epsilon_r + 1}{2} + \frac{\epsilon_r - 1}{2} \left(1 + 12 \frac{h}{W_p}\right)^{-1/2} = \frac{2.2 + 1}{2} + \frac{2.2 - 1}{2} \left(1 + 12 \frac{0.254 \text{ mm}}{4.235 \text{ mm}}\right)^{-1/2} = 1.79 \text{ mm}$$

$$\Delta L = 0.412h \frac{(\epsilon_{\text{reff}} + 0.3) \left(\frac{W}{h} + 0.264\right)}{(\epsilon_{\text{reff}} - 0.258) \left(\frac{W}{h} + 0.8\right)} = 0.412 * 0.254 \frac{(1.79 \text{ mm} + 0.3) \left(\frac{4.235 \text{ mm}}{0.254 \text{ mm}} + 0.264\right)}{(1.79 \text{ mm} - 0.258) \left(\frac{4.235 \text{ mm}}{0.254 \text{ mm}} + 0.8\right)} = 0.138 \text{ mm}$$

$$L_p = \frac{C}{2f_r \sqrt{\epsilon_{\text{reff}}}} - 2 \Delta L = \frac{3 * 10^8 \text{ m/s}}{2 * 28 * 10^9 \text{ Hz} \sqrt{1.79}} - 2 * 0.138 \text{ mm} = 3.469 \text{ mm}$$

$$L_g = L_p + 6h = 3.728 \text{ mm} + 6 * 0.254 \text{ mm} = 5.252 \text{ mm}$$

$$W_g = W_p + 6h = 4.235 \text{ mm} + 6 * 0.254 \text{ mm} = 5.759 \text{ mm}$$

$$Z_a = \frac{90\epsilon_r^2}{\epsilon_r - 1} \left(\frac{L_p}{W_p}\right)^2 = \frac{90 * 2.2^2}{2.2 - 1} \left(\frac{3.728 \text{ mm}}{4.235 \text{ mm}}\right)^2 = 281 \Omega$$

$$Z_{qw} = \sqrt{50 \times 281} = 118 \Omega$$

$$Z_{qw} = \frac{60}{\sqrt{\epsilon_r}} \ln \left(\frac{8h}{W_{qw}} + \frac{W_{qw}}{4h} \right) \Rightarrow 118 = \frac{60}{\sqrt{2.2}} \ln \left(\frac{8 * 0.254 \text{ mm}}{W_{qw}} + \frac{W_{qw}}{4 * 0.254 \text{ mm}} \right)$$

$$W_{qw} = 0.304 \text{ mm}$$

$$L_{qw} = \frac{\lambda_0}{4\sqrt{\epsilon_{reff}}} = \frac{10.7 \text{ mm}}{4\sqrt{1.79}} = 2.002 \text{ mm}$$

$$Z_0 = \frac{120\pi}{\sqrt{\epsilon_{reff}} \left(1.393 + \frac{W_f}{h} + \frac{2}{3} \ln \left(\frac{W_f}{h} + 1.444 \right) \right)} = 50 = \frac{120\pi}{\sqrt{1.79} \left(1.393 + \frac{W_f}{0.254 \text{ mm}} + \frac{2}{3} \ln \left(\frac{W_f}{0.254 \text{ mm}} + 1.444 \right) \right)}$$

$$W_f = 0.783 \text{ mm}$$

$$L_f = \frac{\lambda_0}{4\sqrt{\epsilon_r}} = \frac{10.7}{4\sqrt{2.2}} = 1.804 \text{ mm}$$

In this section, the calculated initial dimensions of the proposed rectangular patch antenna using 28 GHz as the resonant frequency and an r of 2.2 are used. The patch is designed using the overall dimension of the proposed MSPA of 4.235 mm x 3.469 mm x 0.254 mm. The quarter-wave transformer width and length of the feed line are 0.304 mm and 2.002 mm, respectively, and also, the microstrip feed line width and length are 0.783 mm and 1.804 mm, respectively. The values are altered manually, and the effects are observed with the simulator. While tuning the dimension of the antenna parameters, its impact on all the performance metrics is considered by the given design. The initially calculated and optimized dimensions of the rectangular patch antenna are summarized in Table 4.2 below.

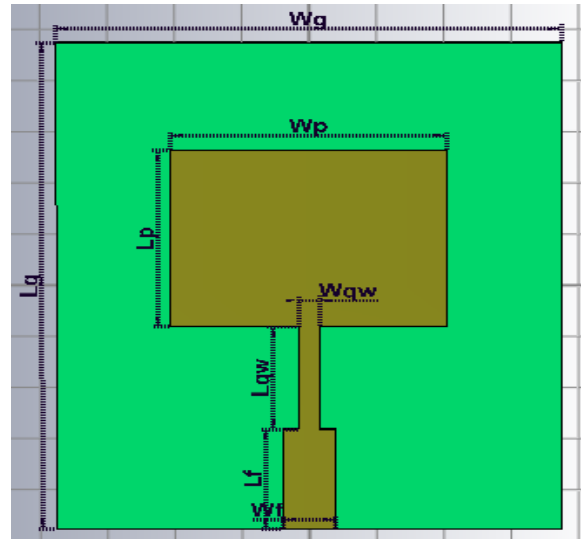


Figure 4. 3: Antenna Design-1

Table 4. 2: Design parameters of Antenna Design-1.

Design Parameters	symbol	Calculated value	Optimized value
Width of Patch	W_p	4.235 mm	4.235 mm
Length of Patch	L_p	3.469 mm	3.335 mm
Width of quarter transformers	W_{qw}	0.304 mm	0.228 mm
Length of quarter transformers	L_{qw}	2.002 mm	2.007 mm
Width of 50Ω feed line	W_f	0.783 mm	0.783 mm
Length of 50Ω feed line	L_f	1.804 mm	1.958 mm
Width of Ground plane	W_g	5.759 mm	5.692 mm
Length of Ground plane	L_g	9.058 mm	8.814 mm
Width of Substrate	W_s	5.759 mm	5.692 mm
Length of Substrate	L_s	9.058 mm	8.814 mm

4.4 Antenna Design-2

It has been discussed in the literature that the creation of slots on the ground plane results in the enhancement of the antenna's bandwidth. So the modified design of the initially designed antenna discussed in the previous section is shown in Figures 4.3a and 4.3b. One triangular slot dimension Ts_1 , Ts_2 , Tw_1 , Tw_2 , Tsw has been slotted on the ground plane. The parameters of this antenna are given in Table 4.3. The overall size of the antenna is 5.692 mm x 8.814 mm x 0.254 mm.

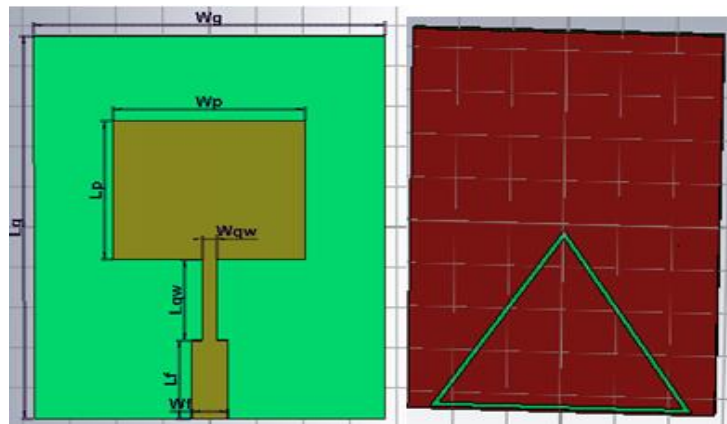


Figure 4. 4: Antenna Design-2 (a) Front view and (b) Back view

Table 4. 3: Design parameters of Antenna Design-2.

Design Parameters	symbols	Optimized value
Width of Patch	W_p	4.105 mm
Length of Patch	L_p	3.51 mm
Width of quarter transformers	W_{qw}	0.228 mm
Length of quarter transformers	L_{qw}	2.007 mm
Width of 50Ω feed line	W_f	0.783 mm
Length of 50Ω feed line	L_f	1.958 mm
Width of Ground plane	W_g	5.692 mm
Length of Ground plane	L_g	8.814 mm
Width of Substrate	W_s	5.692mm
Length of Substrate	L_s	8.814 mm
Rectangular slot width of ground plane	G_{sw}	1 mm
Rectangular slot length of ground plane	G_{sl}	1 mm
Triangular slot outer length of ground plane	T_{s1}	2.8 mm
Triangular slot inner length of ground plane	T_{s2}	2.6 mm
Triangular slot outer width of ground plane	T_{sw1}	2.8 mm
Triangular slot inner width of ground plane	T_{sw2}	2.6 mm
Triangular slots width of ground plane	T_{sw}	0.2 mm

4.5 Antenna Design-3

In order to enhance the impedance bandwidth, the formerly antenna design-2 has been modified as shown in Figure 4.5. The L_p has been changed and four rectangular slots on ground plane have been added to the design. The lengths of the rectangular slots are denoted by G_{sl} while their widths are represented by G_{sw} . The parameters of the antenna design-3 are given in Table 4.4. The overall size of the antenna is 5.962 mm x 8.814 mm x 0.254 mm.

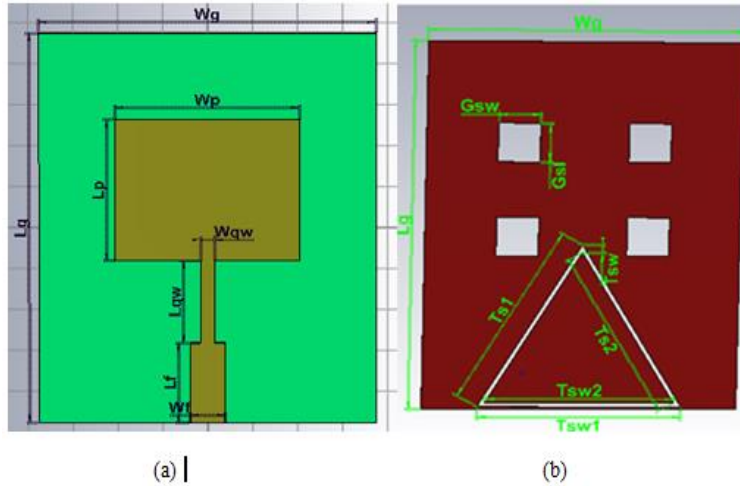


Figure 4. 5: Antenna Design-3 (a) Front View and (b) Back View

Table 4. 4: Design parameters of the Antenna Design-3.

Design Parameters	symbols	Optimized value
Width of Patch	W_p	4.235 mm
Length of Patch	L_p	3.55 mm
Width of quarter transformers	W_{qw}	0.228 mm
Length of quarter transformers	L_{qw}	2.007 mm
Width of 50Ω feed line	W_f	0.783 mm
Length of 50Ω feed line	L_f	1.958 mm
Width of Ground plane	W_g	5.692 mm
Length of Ground plane	L_g	8.814 mm
Width of Substrate	W_s	5.692 mm
Length of Substrate	L_s	8.814 mm
Rectangular slot width of ground plane	G_{sw}	1 mm
Rectangular slot length of ground plane	G_{sl}	1 mm
Triangular slot outer length of ground plane	T_{s1}	2.8 mm
Triangular slot inner length of ground plane	T_{s2}	2.6 mm
Triangular slot outer width of ground plane	T_{sw1}	2.8 mm
Triangular slot inner width of ground plane	T_{sw2}	2.6 mm
Triangular slots width of ground plane	T_{sw}	0.2 mm

4.6 Design of the Proposed Antenna

The width of the substrate and ground of the aforementioned 3rd antenna has been increased from 5.692 mm to 7.6 mm and length of substrate and ground plane has been decreased by 8.814 mm to 8.8 mm. The length of the radiating patch antenna has been increased from 3.55mm to 3.6 mm and width of radiated patch antenna has been decreased from 4.235 mm to 4.105 mm. The quarter wave transformer width has been decreased from 0.228 mm to 0.16 mm. The previous antenna has been modified to achieve improvement in the bandwidth as well as other characteristics of the antenna. So, two slots have been etched on the radiating patch and five slots on ground plane. Four equal rectangular slots have been created in ground plane which width and length of each one is represented by $G_{sw} \times G_{sl}$. One triangular slot on the ground plane dimensions is represented by T_{s1} , T_{s2} , T_{w1} , T_{w2} , and T_{sw} . Two circular slots of equal radius r have been created on upper sides of the radiating patch antenna as shown in Figure 4.6. The parameters that have been changed are given in Tables 4.6. The remaining parameters are exactly the same as 3rd antenna. The size of the substrate as well as ground plane is 7.6 mm x 8.8 mm x 0.254 mm.

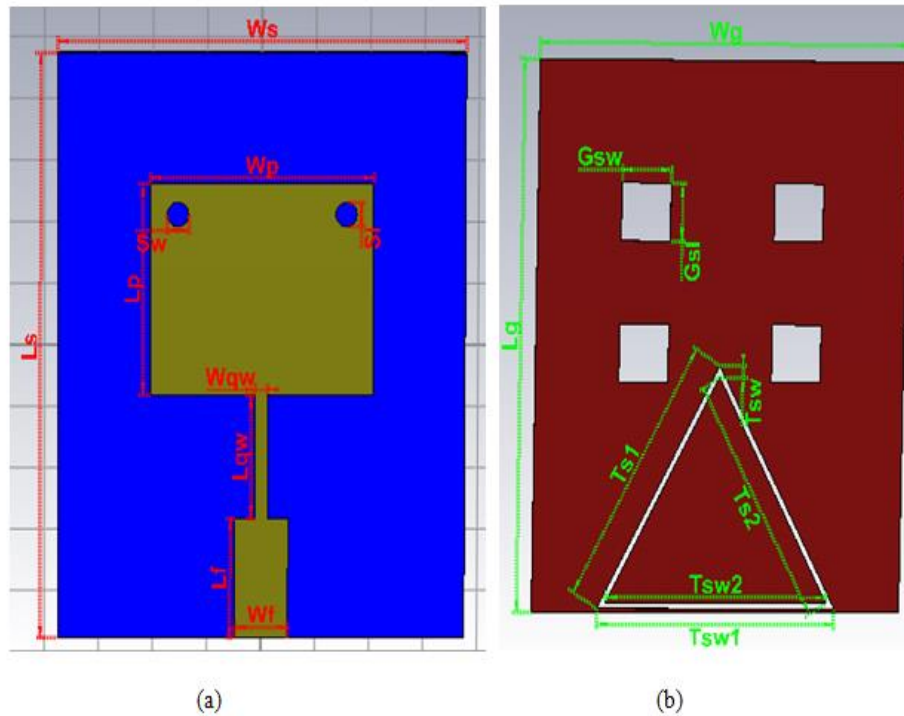


Figure 4. 6: Proposed of the proposed antenna where (a) front view and (b) back view

Table 4. 5: Design parameters of the proposed antenna

Design Parameters	symbols	Optimized value
Width of Patch	W_p	4.105 mm
Length of Patch	L_p	3.6 mm
Width of quarter transformers	W_{qw}	0.16 mm
Length of quarter transformers	L_{qw}	2.007 mm
Width of 50Ω feed line	W_f	0.783 mm
Length of 50Ω feed line	L_f	1.958 mm
Width of Ground plane	W_g	7.6 mm
Length of Ground plane	L_g	8.8 mm
Width of Substrate	W_s	7.6 mm
Length of Substrate	L_s	8.8 mm
Circular slot of patch width	S_w	0.2 mm
Circular slot of patch length	S_L	0.2 mm
Rectangular slot width of ground plane	G_{sw}	1 mm
Rectangular slot length of ground plane	G_{sl}	1 mm
Triangular slot outer length of ground plane	T_{s1}	2.8 mm
Triangular slot inner length of ground plane	T_{s2}	2.6 mm
Triangular slot outer width of ground plane	T_{sw1}	2.8 mm
Triangular slot inner width of ground plane	T_{sw2}	2.6 mm
Triangular slots width of ground plane	T_{sw}	0.2 mm

4.5 Design of 2x1 slotted rectangular MSPA Arrays

A single-element slotted rectangular patch antenna is designed and extended to be a 2x1-element slotted patch array antenna as shown in Figure4.7. This model was introduced for the purposes of enhancing the performance of the antenna, such as increasing its gain, directivity scanning the beam of an antenna system, and other functions that are difficult to achieve in the case of a single element. A microstrip line of 1:2 power dividers is used to feed the two antennas, and hence the line widths are adjusted according to the power division. The distance between the two patches is d.

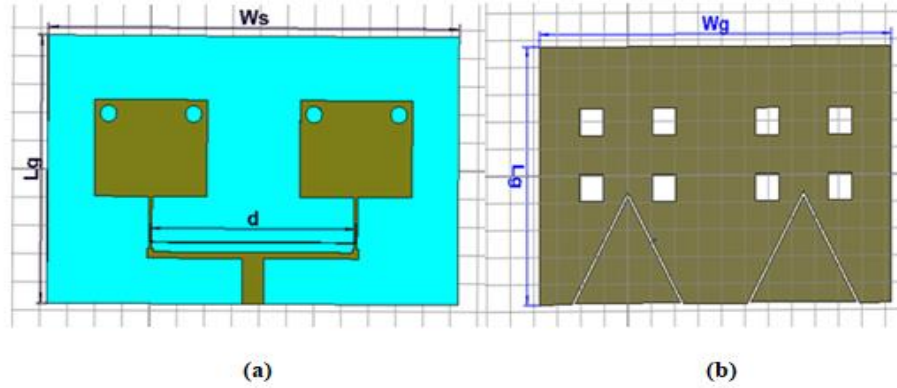


Figure 4. 7:2 x 1 array of slotted antenna (a) front view and (b) back view

Table 4. 6: Dimension of 2x1 Rectangular Patches Array Antenna.

Design Parameters	Symbol	Optimized value
Width of Patch	W_p	4.105 mm
Length of Patch	L_p	3.6 mm
Width of quarter transformers	W_{qw}	0.024 mm
Length of quarter transformers	L_{qw}	2.08 mm
Width of 50Ω feed line	W_f	0.783 mm
Length of 50Ω feed line	L_f	1.958 mm
Width of 70Ω matching line	W_{ml}	3.1 mm
Length of 70Ω matching line	L_{ml}	0.808 mm
Width of Ground plane	W_g	12.4 mm
Length of Ground plane	L_g	10.5 mm
Width of Substrate	W_s	12.4 mm
Length of Substrate	L_s	10.5 mm
Distance between two patch center to center	d	6.2
Circular slot of patch width	S_w	0.5 mm
Circular slot of patch length	S_L	0.5 mm
Rectangular slot width of ground plane	G_{sw}	1 mm
Rectangular slot length of ground plane	G_{SL}	1 mm

Design Parameters	Symbol	Optimized value
Triangular slot outer length of ground plane	T_{S1}	2.8 mm
Triangular slot inner length of ground plane	T_{S2}	2.6 mm
Triangular slot outer width of ground plane	T_{Sw1}	2.8 mm
Triangular slot inner width of ground plane	T_{Sw2}	2.6 mm
Triangular slots width of ground plane	T_{Sw}	0.2 mm

4.5 Design of 4x1 slotted rectangular MSPA Arrays

In this thesis, the corporate feed network is chosen for designing four-element array networks. The array antenna consists of a branching network of two-way power dividers. Quarter-wave transformers (QWT) are used to match the lines to the lines. The design of a single element slotted rectangular patch antenna is extended to 4x1 linear phase arrays, as shown in the figures (4.8 (a) and (b)) below, and Table 4.5 shows the dimensions of a 4x1 slotted array antenna. Referring to the calculation of the distance between the elements, which is half the wavelength ($\lambda/2 = d$).

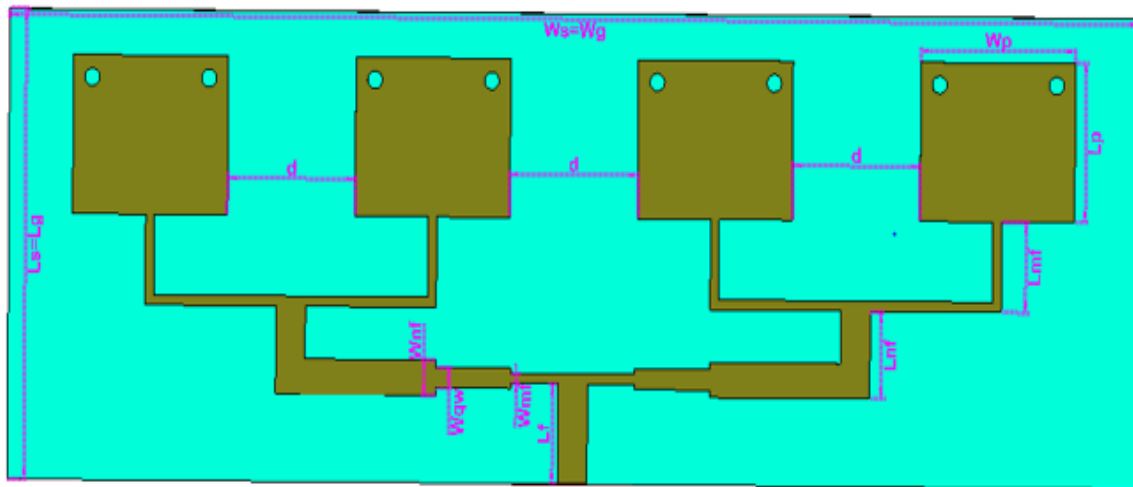


Figure 4. 8a: Constructional Details of 4 x 1 array of front view

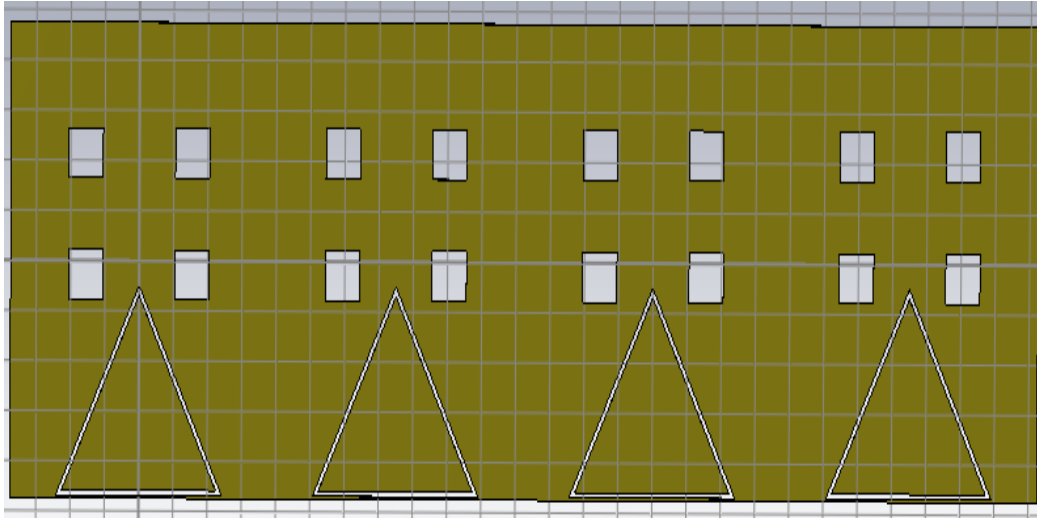


Figure 4. 8b: Constructional Details of 4 x 1 array of ground plane

Table 4. 7: Dimension of Rectangular Patches Array Antenna.

Design Parameters	Symbol	Optimized value
Width of Patch	W_p	4.105 mm
Length of Patch	L_p	3.6 mm
Width of quarter transformers	W_{qw}	0.304 mm
Length of quarter transformers	L_{qw}	2.082 mm
Width of 50Ω feed line	W_f	0.783 mm
Length of 50Ω feed line	L_f	1.842 mm
Width of 100Ω matching line	W_{mf}	0.228 mm
Length of 100Ω matching line	L_{mf}	2.02 mm
Width of 70Ω matching line	W_{ml}	0.391 mm
Length of 70Ω matching line	L_{ml}	1.987 mm
Width of Ground plane	W_g	24.8 mm
Length of Ground plane	L_g	11.5 mm
Width of Substrate	W_s	24.8 mm
Length of Substrate	L_s	11.5 mm
Distance between two patch	d	6.2

Design Parameters	Symbol	Optimized value
Circular slot of patch width	S_w	0.5 mm
Circular slot of patch length	S_L	0.5 mm
Rectangular slot width of ground plane	G_{sw}	1 mm
Rectangular slot length of ground plane	G_{sl}	1 mm
Triangular slot outer length of ground plane	T_{s1}	2.8 mm
Triangular slot inner length of ground plane	T_{s2}	2.6 mm
Triangular slot outer width of ground plane	T_{sw1}	2.8 mm
Triangular slot inner width of ground plane	T_{sw2}	2.6 mm
Triangular slots width of ground plane	T_{sw}	0.2 mm

Simulation of the proposed antenna's structure is performed using the simulation tool called CST Micro Studio 2019.

CHAPTER FIVE

5. Simulation results and Discussion

5.1 Introduction

The simulation results and discussion of the proposed antenna and arrays are presented in this section. To analyze the intended antenna, we used CST software to simulate the proposed antennas design. Different performance indicators are utilized to access an antenna's features. Among these is the bandwidth, gain, directivity, VSWR, return loss and radiation efficiency. The size of the return loss is used to quantify the matching quality between the radiating patch and the feed point. The radiation pattern is another characteristic that is frequently used to characterize the MSPA. The angular strength of power radiated from the antenna is shown by the plot of the far-field pattern. It is used to demonstrate the directivity and gain of a given antenna at a given point in space. And finally, the results will be discussed in term of the selected parameters for comparison.

5.2 Antenna Design-1 Simulation Results

The antenna's dual band operation is illustrated in Figure 5.1. In the first band, a bandwidth of 0.854 GHz was attained, while in the second band, a bandwidth of 1.301 GHz was reached. The first band's lower frequency is 27.582 GHz, while its higher frequency is 28.436 GHz. The second band, on the other hand, has a lower frequency of 43.591 GHz and a higher frequency of 44.892 GHz. Return losses of -33.667dB at the center frequency of 28GHz in the first band and return losses of -24.44 dB at the center frequency of 44.192GHz in the second band have been achieved.

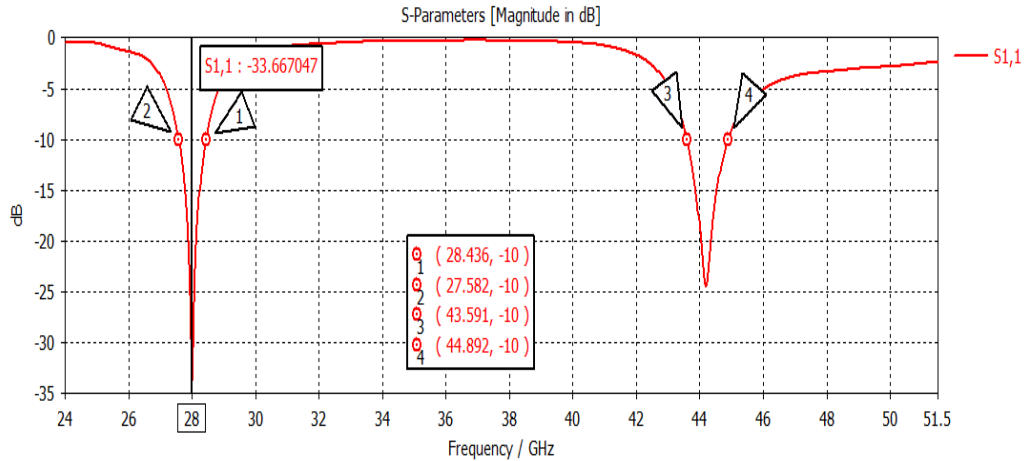


Figure 5. 1: Reflection Coefficient of Antenna Design-1

The VSWRs of 1.0425 and 1.1317 have been obtained at the center frequencies of 28 GHz and 44.192 GHz, respectively. It shows that mismatch loss has been significantly reduced. Definitely, the ratio is less than 2 in the entire working band.

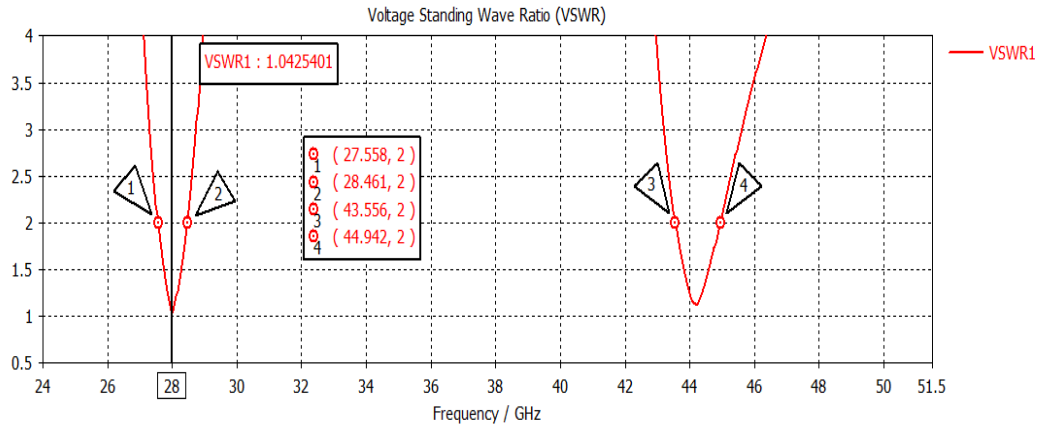


Figure 5. 2: VSWR of Antenna Design-1

The 3D radiation patterns at the center frequencies of 28GHz and 44.192GHz are shown in Figures 5.3a and 5.3b respectively. Gains of 7.1dBi and 7.66dBi have been obtained at the center frequencies of 28GHz and 44.192GHz respectively. Radiation efficiencies of -0.4652dB (89.84%) and -0.1872dB (95.78%) have been achieved at the center frequencies of 28GHz and 44.192GHz respectively.

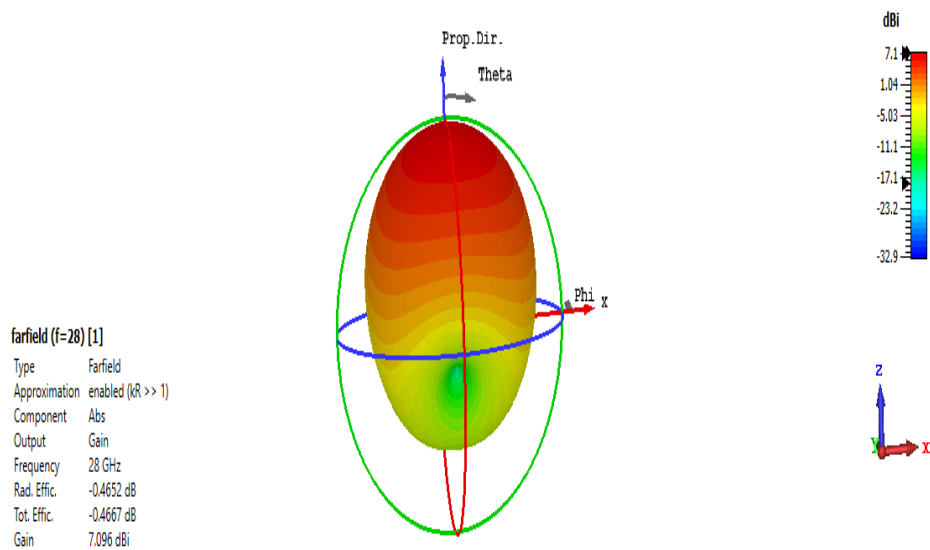


Figure 5. 3a: 3D Radiation Pattern of Antenna Design-1

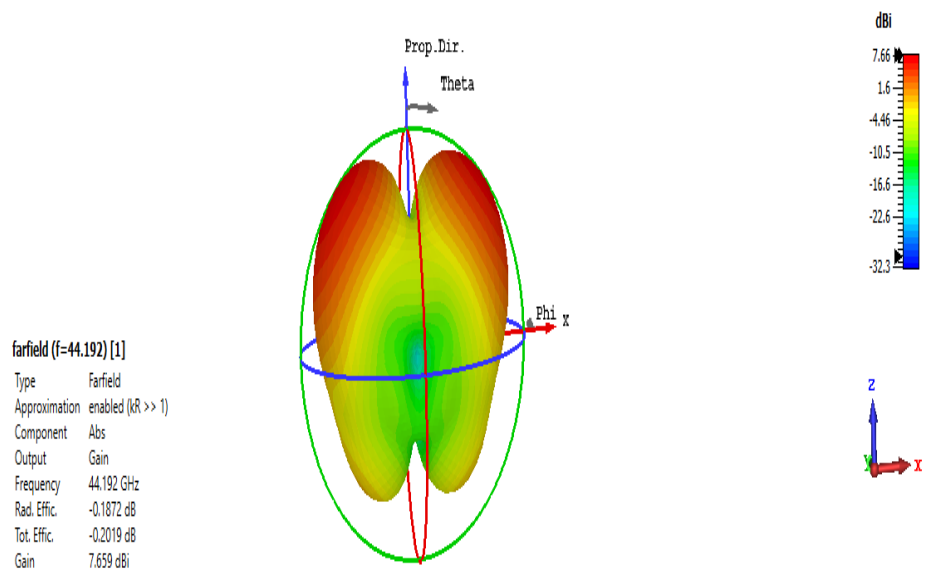


Figure 5.3b: 3D Radiation Pattern of Antenna Design-1

The half-power beam widths of 72.8° and 41.0° have been achieved at the center frequencies of 28GHz and 44.192GHz, respectively. The side lobe levels of 13.3dB and -5.7dB have been achieved at frequencies of 28GHz and 44.192GHz, respectively. They are observed in these 2D radiation patterns in Figures 5.4a and 5.4b, respectively.

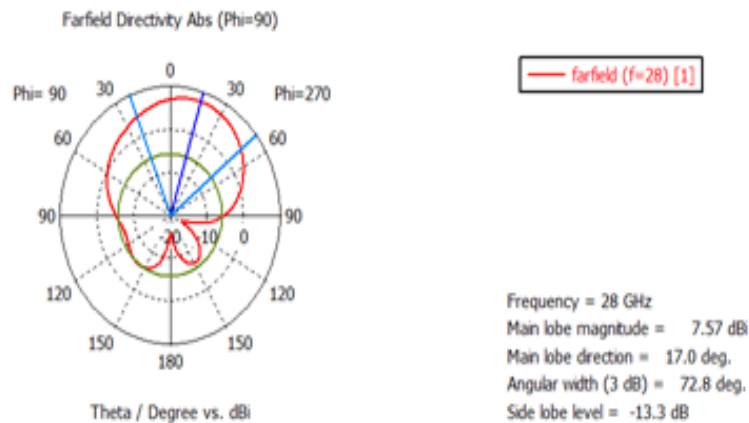


Figure 5. 4b: 2D Radiation Pattern of Antenna Design-1

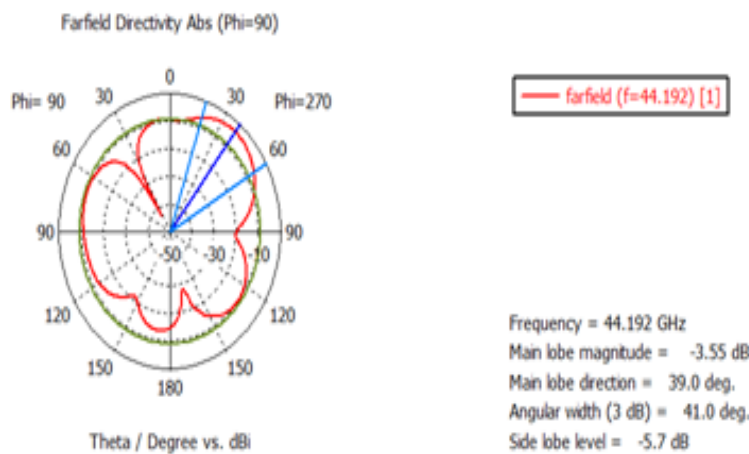


Figure 5.4b: 2D Radiation Pattern of Antenna Design-1

5.3 Antenna Design-2 Simulation Results

The tri-band operation of the antenna is shown in Figure 5.1. A bandwidth of 1.042GHz in the first band, a bandwidth of 6.587GHz in the second band, and a bandwidth of 2.774GHz in the third band have been achieved. The lower frequency of the first band is 27.582 GHz, and its higher frequency is 28.624GHz. The lower frequency of the second band is 37.337GHz, and its higher frequency is 43.933GHz. However, the lower frequency of the third band is 46.142 GHz and its higher frequency is 48.953 GHz. Return losses of -26.127dB at the center frequency of the first band, return losses of -21.600dB at the center frequency of the second band, and return losses of -20.446dB at the center frequency of the third band have been achieved.

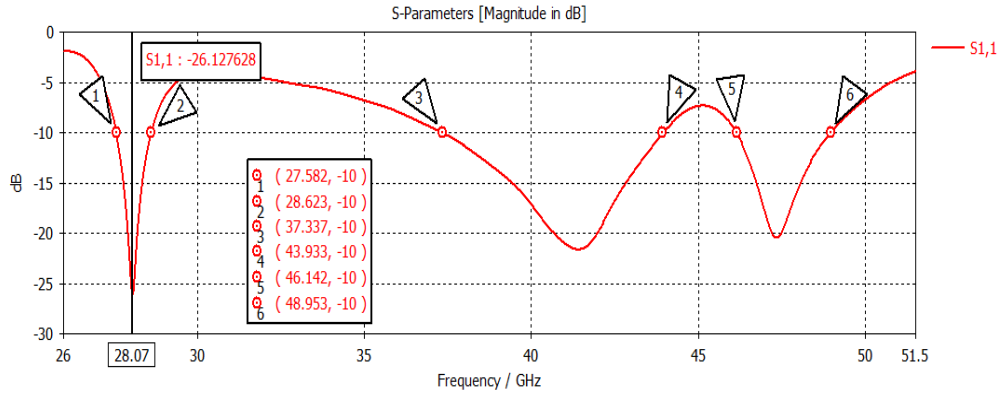


Figure 5. 5: Reflection Coefficient of Antenna Design-2.

The diagram of VSWR is shown in Figure 5.6. This ratio is less than 2 in the entire operating bandwidth and the values of 1.1039, 1.1814, and 1.2099 have been obtained at the center frequencies of 28.07GHz, 41.408GHz, and 47.347GHz, respectively. Definitely, the ratio is unquestionably less than 2 in the entire working bands.

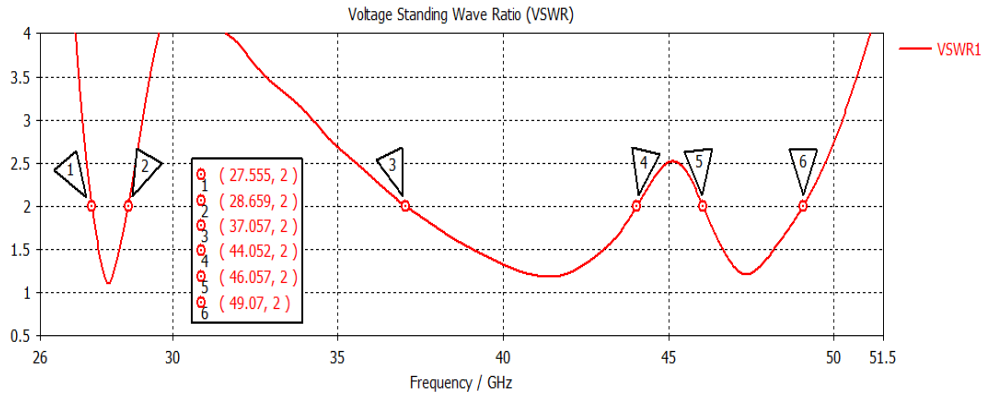


Figure 5. 6: VSWR of Antenna Design-2

Another feature that is usually used to describe the MSPA is its radiation pattern. The plot of the far-field pattern shows the angular strength of the power radiated by the antenna. It's used to show the directivity and gain of an antenna at a specific location in space. The 3D radiation patterns at the center frequencies of 28.07GHz, 41.408 and 47.347GHz are shown in Figures 5.7a, 5.7b, and 5.7c, respectively. Gains of 7.28dBi, 2.24dBi, and 6.92dBi have been achieved at the center frequencies of 28.07GHz, 41.408GHz, and 47.347GHz, respectively. Radiation efficiencies of -0.4186dB (90.81%), -1.6501 (68.388%) and -0.1872dB (94.11%) have been achieved at the center frequencies of 28.08GHz, 41.408GHz and 47.347GHz, respectively.

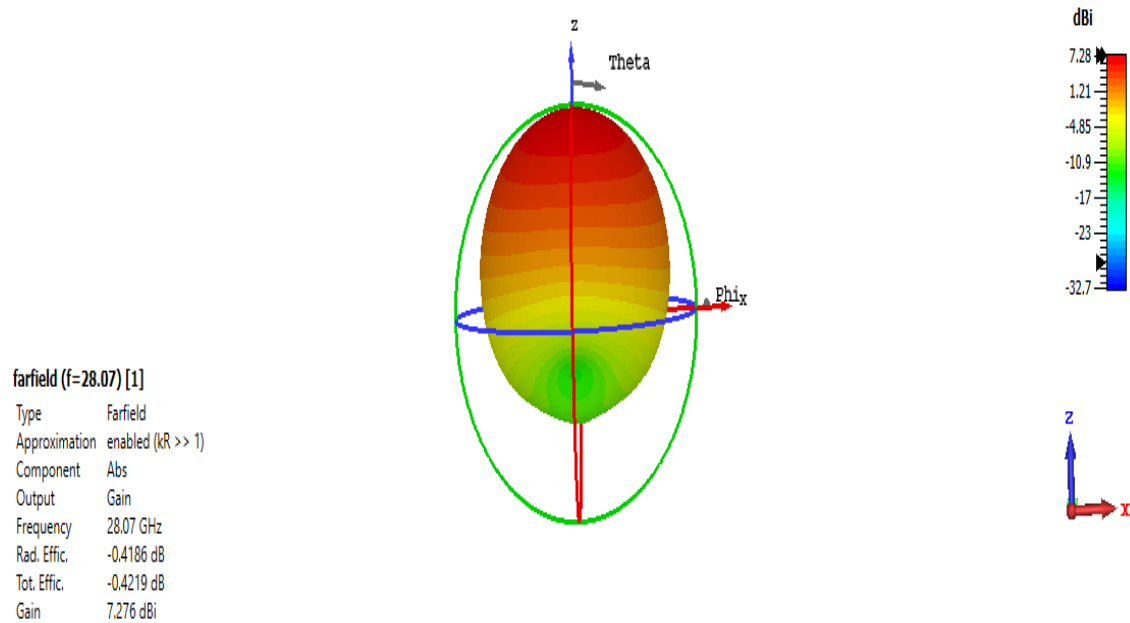


Figure 5. 7a: 3D Radiation Pattern of Antenna Design-2

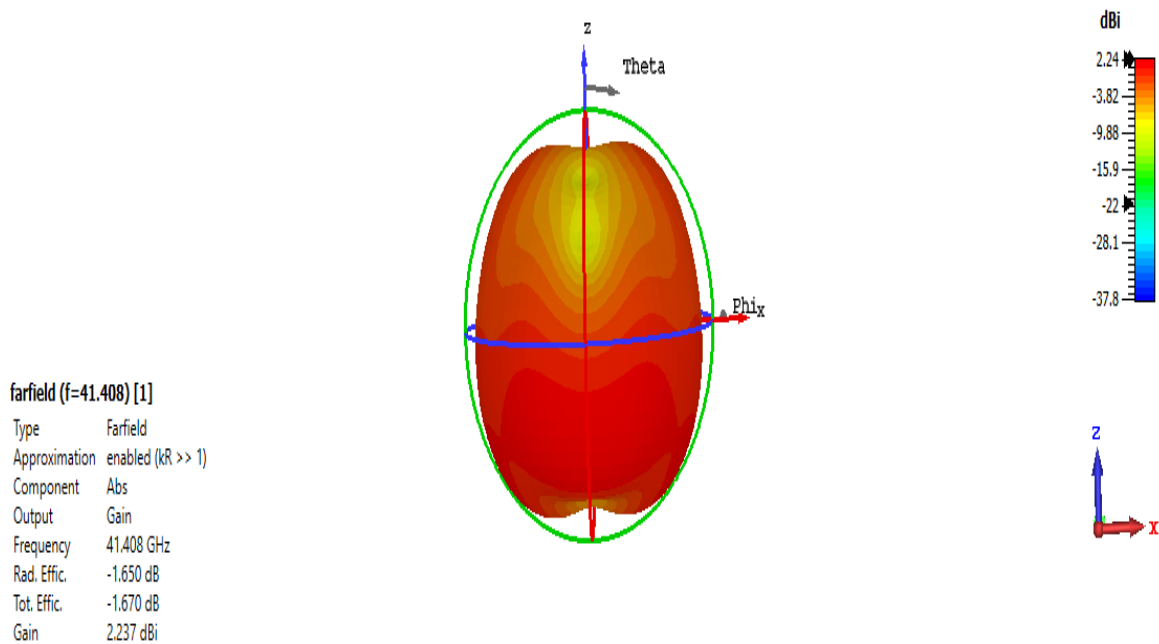


Figure 5.7b: 3D Radiation Pattern of Antenna Design-2

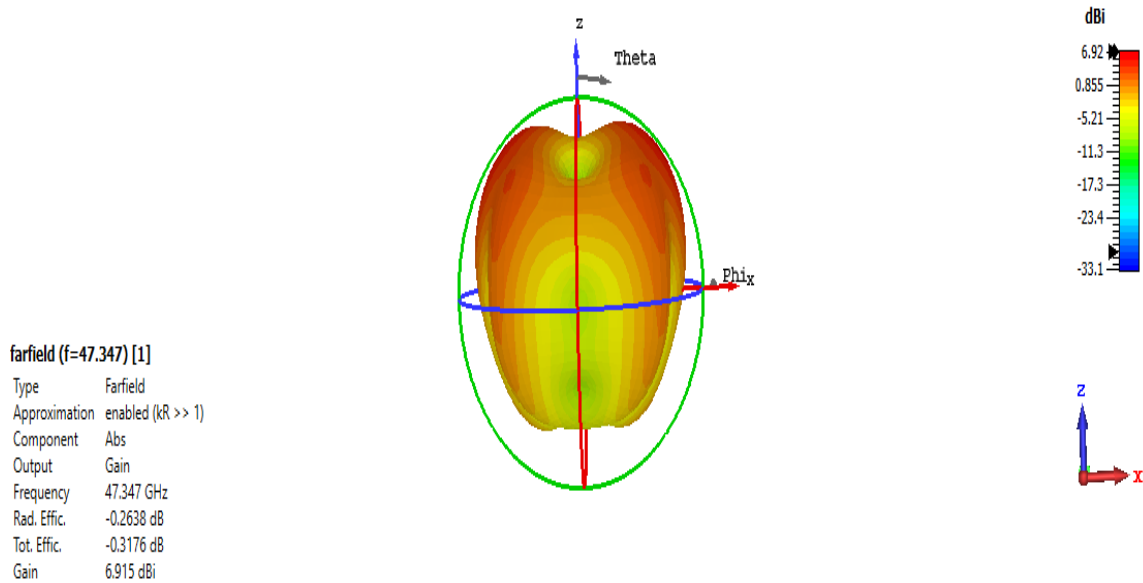


Figure 5.7c: 3D Radiation Pattern of Antenna Design-2

The 2D angular width (3 dB) of 69.3°, 53.4°, and 34.2° has been achieved at the center frequencies of 28.07GHz, 41.408GHz, and 47.347GHz, respectively. The side lobe levels of 14.2dB, -2.9dB, and -1.3dB have been achieved at frequencies of 28.07GHz, 41.408 GHz, and 44.192GHz, observed in these 2D radiation patterns in Figures 5.8a, 5.8b, and 5.8c, respectively.

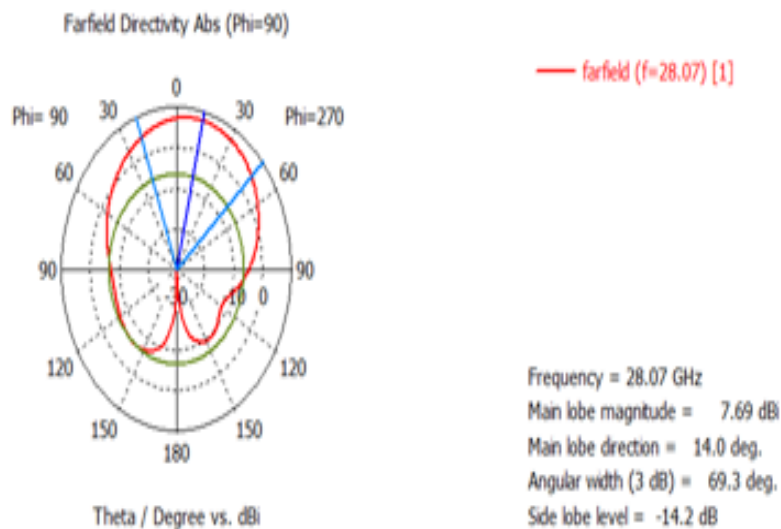


Figure 5. 8a: 2D Radiation Pattern of Antenna Design-2

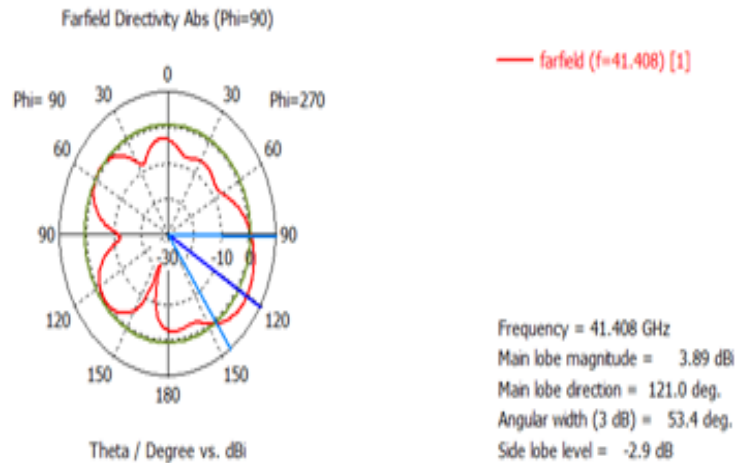


Figure 5.8b: 2D Radiation Pattern of Antenna Design-2

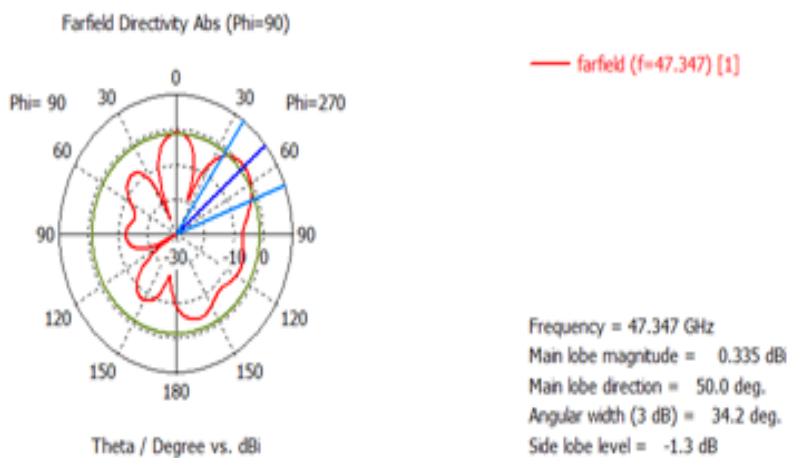


Figure 5.8c: 2D Radiation Pattern of Antenna Design-2

5.4 Antenna Design-3 Simulation Results

As shown in Figure 4.5 and the simulation results discussed in this section, there are five rectangular and one triangular slot on the ground plane of the antenna design. The dual band operation of the antenna is shown in Figure 5.1. A bandwidth of 1.266GHz in the first band and a bandwidth of 12.913GHz in the second band have been achieved. The lower frequency of the first band is 27.455GHz, and its higher frequency is 28.721GHz. However, the lower frequency of the second band is 37.42 GHz and its higher frequency is 50.333 GHz. The fractional

bandwidths of 4.511% for the first band and 29.685% for the second band have been obtained. Return losses of -30.202dB at the center frequency of the first band and a return loss of -28.754dB at the center frequency of the second band have been achieved.

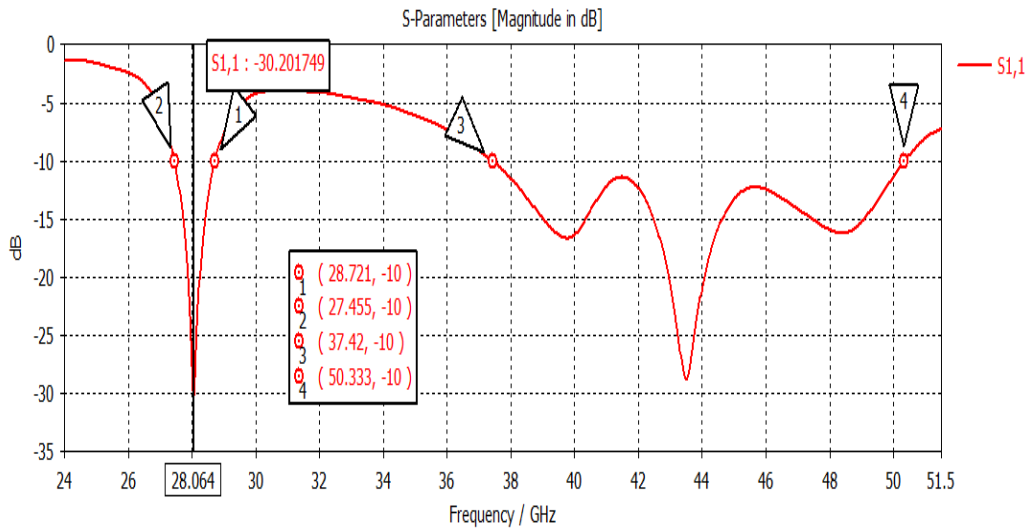


Figure 5. 9: Reflection Coefficient of Antenna Design-3.

The VSWRs of 1.0425 and 1.1317 have been obtained at the center frequencies of 28 GHz and 44.192 GHz, respectively. It shows that mismatch loss has been significantly reduced.

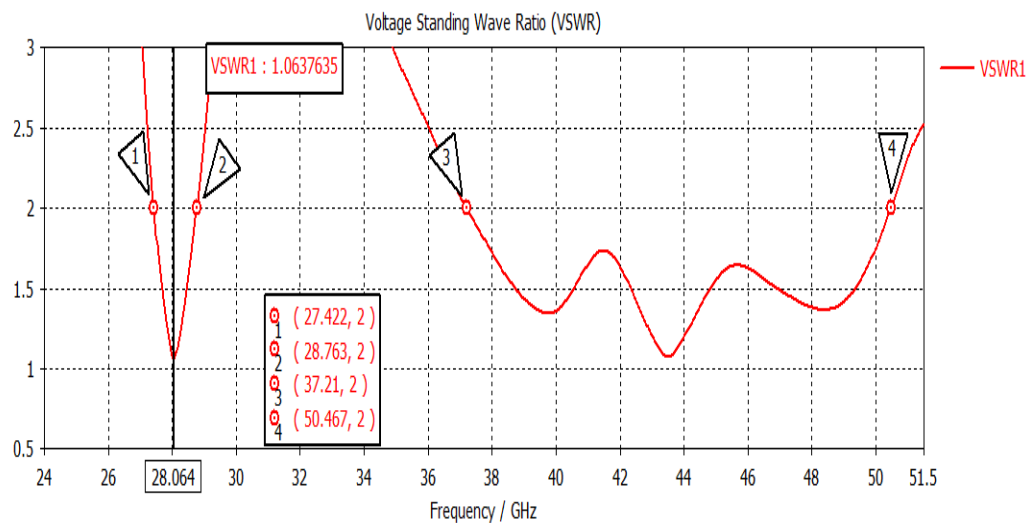


Figure 5. 10: VSWR of Antenna Design-3.

The 3D radiation patterns at the center frequencies of 28.064GHz and 43.499GHz are shown in Figures 5.11a and 5.11b, respectively. Gains of 7.4dBi and 4.2dBi have been obtained at the

center frequencies of 28.064GHz and 44.192GHz, respectively. Radiation efficiencies of -0.2246dB (94.96%) and -0.8397dB (82.42%) have been achieved at the center frequencies of 28.064GHz and 43.499GHz, respectively.

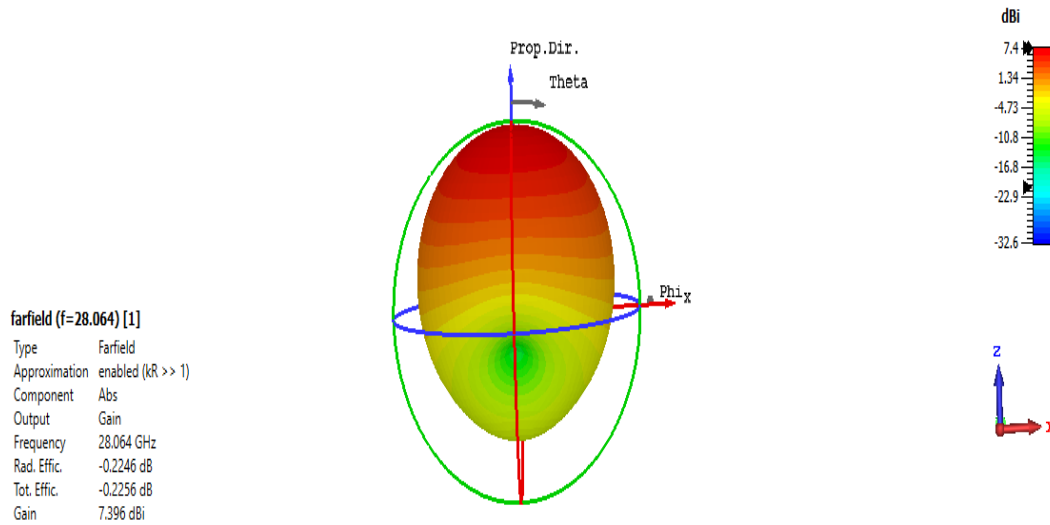


Figure 5. 11a: 3D Radiation Pattern of Antenna Design-3

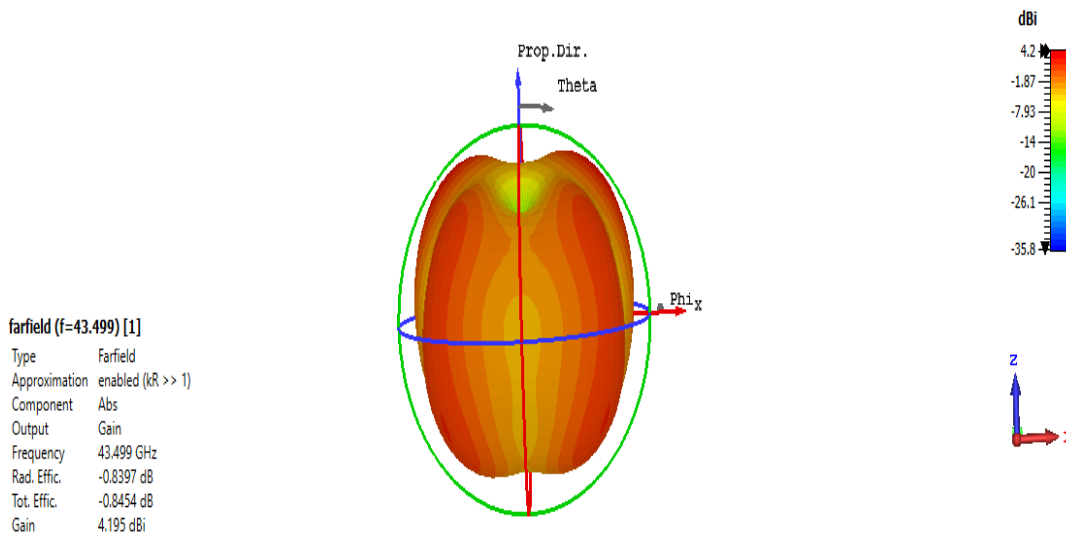


Figure 5.11b: 3D Radiation Pattern of Antenna Design-3

The half-power beam widths of 66.2° and 124.7° have been achieved at the center frequencies of 28.064GHz and 44.192GHz, respectively. The side lobe levels of 12.2dB and -1.6dB have been

achieved at frequencies of 28.064GHz and 43.499GHz, respectively. They are observed in these 2D radiation patterns in Figures 5.12a and 5.12b, respectively.

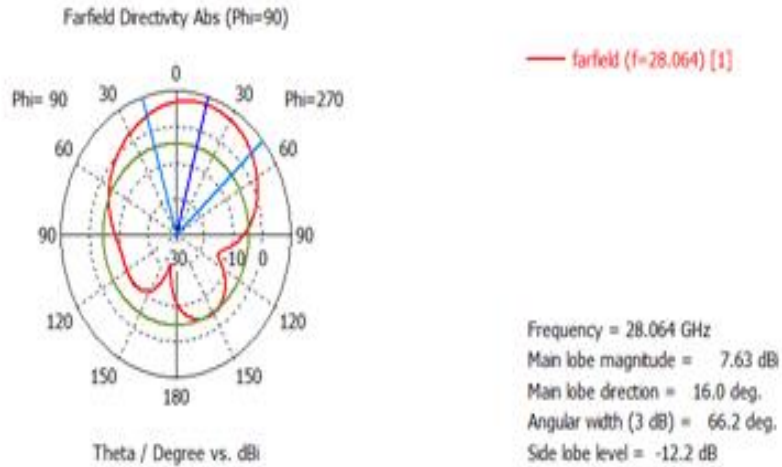


Figure 5. 12a: 2D Radiation Pattern of Antenna Design-3

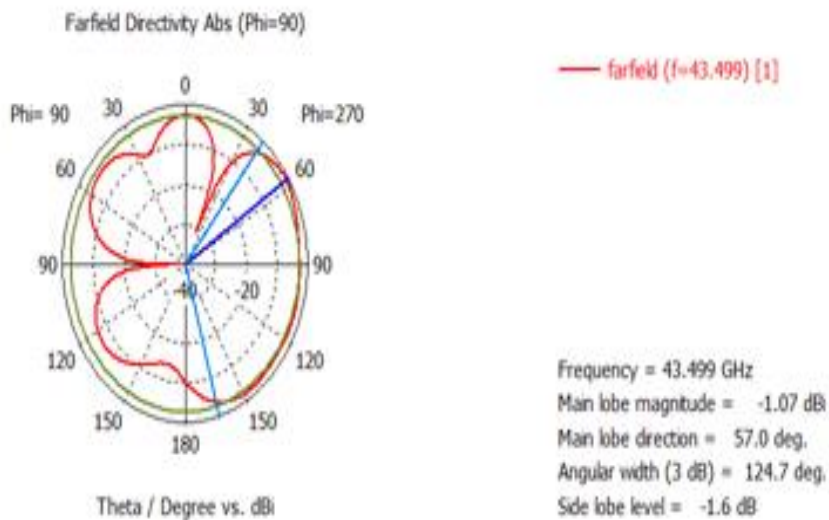


Figure 5.12b: 2D Radiation Pattern of Antenna Design-3

5.5 Design of the Proposed Antenna-4 Simulation Results

The proposed single element has two circular slots on the radiated patch and one triangular slot with four rectangular slots on the ground plane, as shown in figure 4.6 and the simulation results have been discussed in this section. The reflection coefficient of the antenna is shown in Figure 5.13. The BW's final proposed single-element antenna has been enhanced to 23.858GHz. The lower frequency of the bandwidth is 27.412 GHz and the higher frequency is 51.27 GHz. A return loss of -46.294814 dB has been achieved at the center frequency of 28.001 GHz. A FBW of 85.207% has been obtained by this final design.

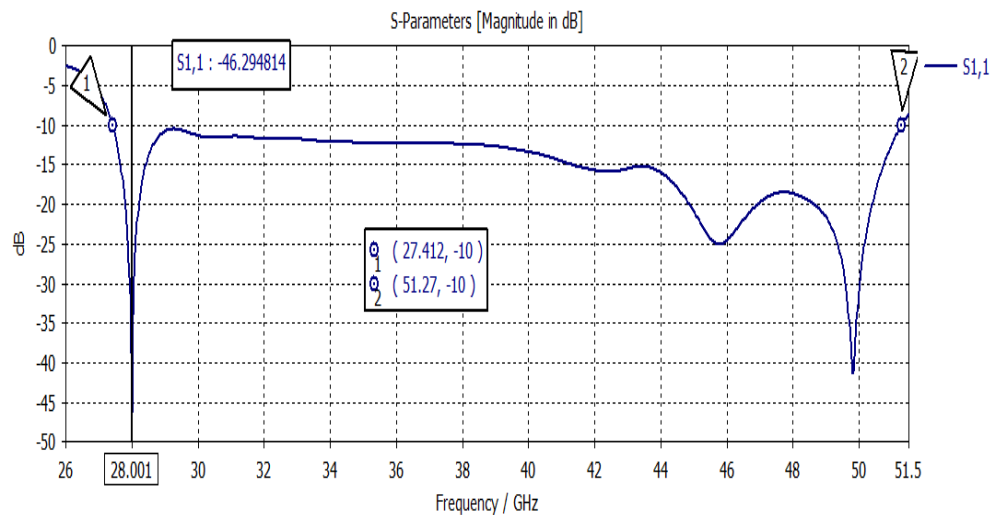


Figure 5. 13: Reflection Coefficient of ProposedAntenna-4

The VSWR of the antenna is shown in Figure 5.14. The ratio between 1 and 2 has been achieved in the entire operating band of the proposed antenna-4. As discussed earlier, this ratio would be equal to 1 if the antenna is perfectly matched. As the return loss at the center frequency is 46.295dB, this ratio is approaching 1 at this frequency. The VSWR of this antenna at the center frequency is less than that of the above-designed antennas. A VSWR of 1.009736 has been obtained at the center frequency of 28.001GHz.

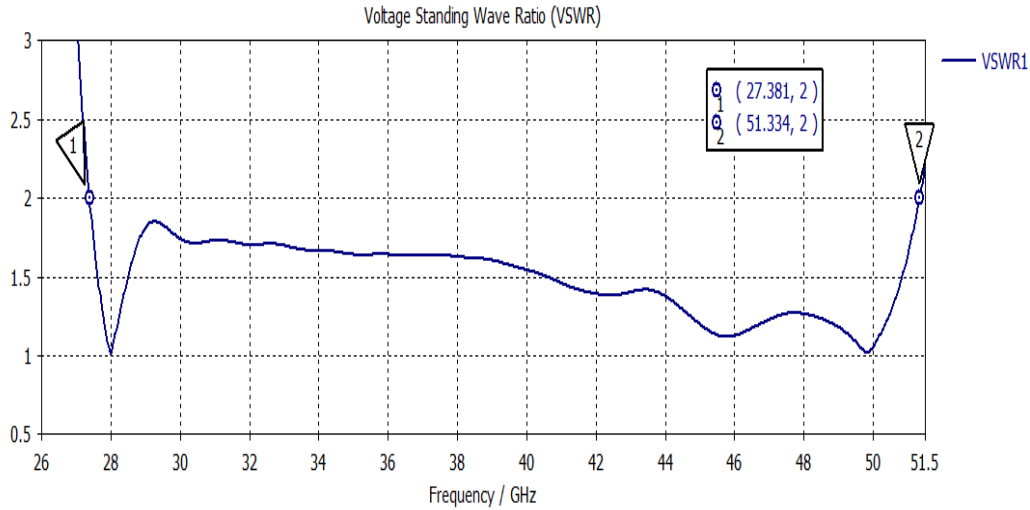


Figure 5. 14: VSWR of ProposedAntenna-4

The radiation pattern is another characteristic that is frequently used to characterize the MSPA. The angular strength of the power radiated from the antenna is shown by the plot of the far-field pattern. It is used to demonstrate the directivity and gain of a given antenna at a given point in space. The gain and radiation efficiency are 7.27 dBi and (-0.3804dB) 91.62%, respectively, as shown in Figure 5.15a. Similarly, as shown in Figure 5.15b, the 2D side lobe level and half-power beam width are 11.1 dB and 69.6 degrees, respectively.

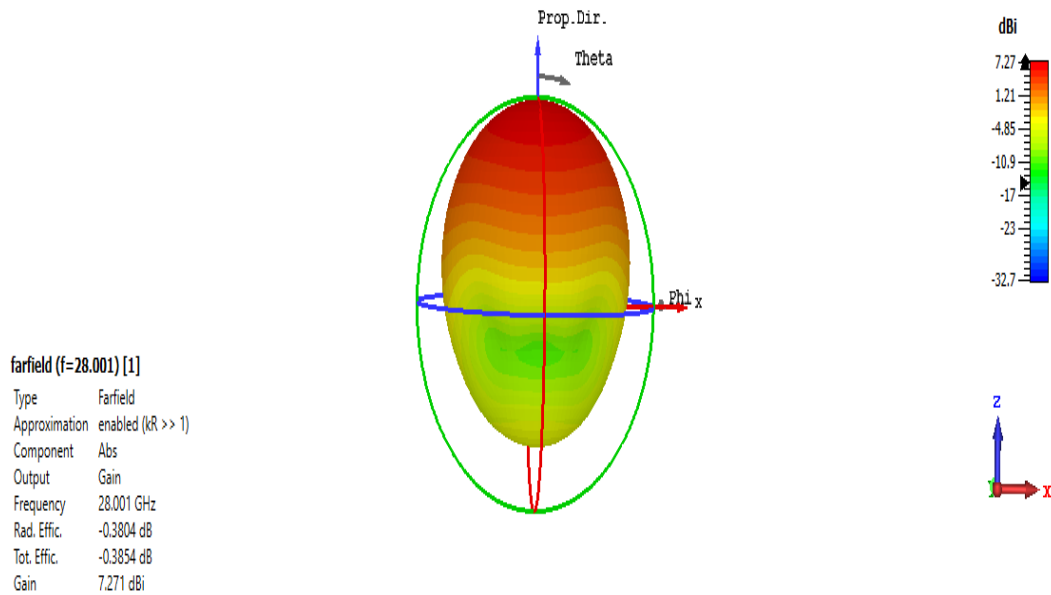


Figure 5. 15a: 3D Radiation Pattern of Proposed Antenna Design-4

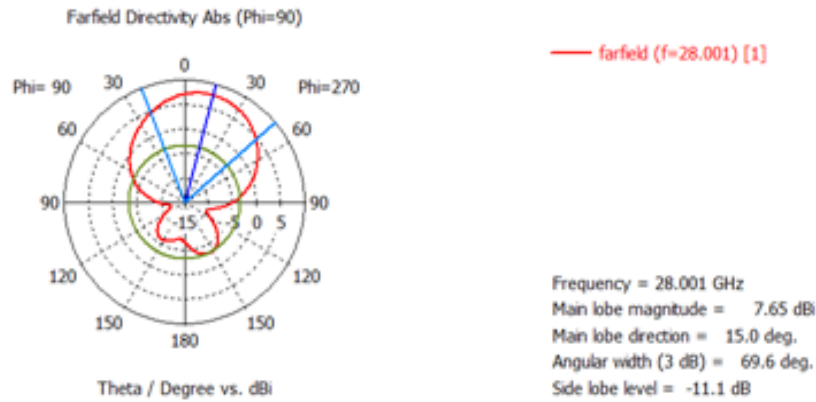


Figure 5.15b: 2D Radiation Pattern of Proposed Antenna Design-4

5.6: Proposed 2x1 slotted antenna arrays

As shown in Figure 4.7 and the simulation results discussed in this section, the slotted 2x1 array antenna design. The dual band operation of the antenna is shown in Figure 5.16. A bandwidth of 9.554GHz in the first band and a bandwidth of 11.465GHz in the second band have been achieved. The lower frequency of the first band is 27.509GHz, and its higher frequency is 37.063GHz. However, the lower frequency of the second band is 39.621 GHz and its higher frequency is 51.086 GHz. Return losses of -41.238dB at the center frequency of the first band and a return loss of -26.878dB at the center frequency of the second band have been achieved.

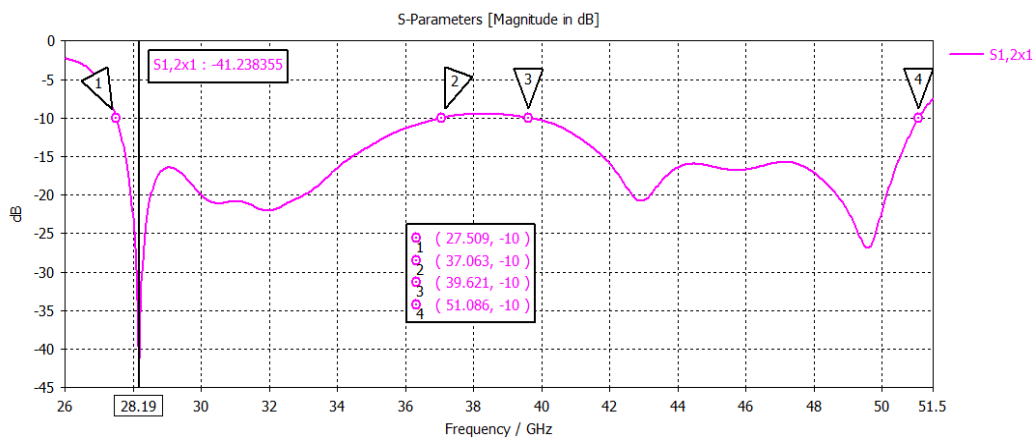


Figure 5. 16: Reflection Coefficient of Proposed 2x1 arrays

The 3D radiation patterns at the center frequencies of 28.19GHz and 49.578GHz are shown in Figures 5.17a and 5.17b, respectively. Gains of 9.93dBi and 9.53dBi have been obtained at the center frequencies of 28.19GHz and 49.578GHz, respectively.

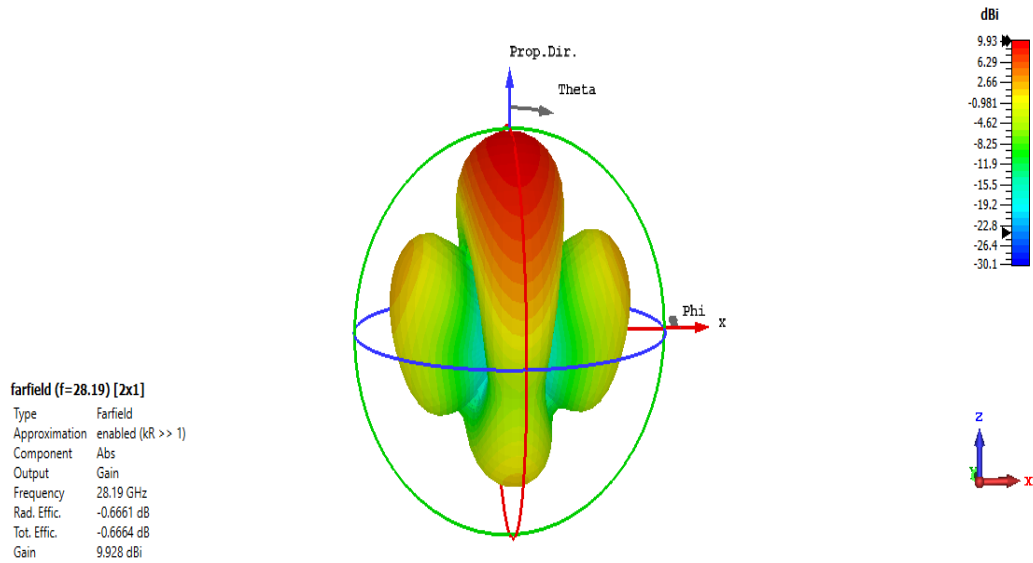


Figure 5. 17a: 3D Radiation Pattern of Proposed 2x1 array

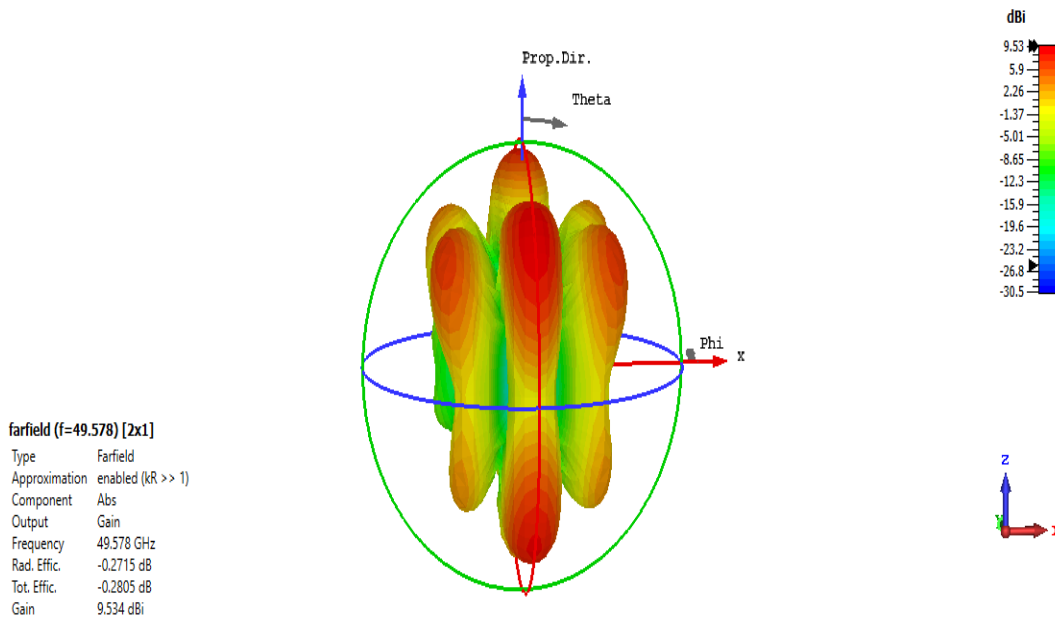


Figure 5.17b: 3D Radiation Pattern of Proposed 2x1 array

The half-power beam widths of 67.3° and 38.1° have been achieved at the center frequencies of 28.19GHz and 49.578GHz, respectively. The side lobe levels of -9.6dB and -0.8dB have been

achieved at frequencies of 280.64GHz and 43.499GHz, respectively. They are observed in these 2D radiation patterns in Figures 5.18a and 5.18b, respectively.

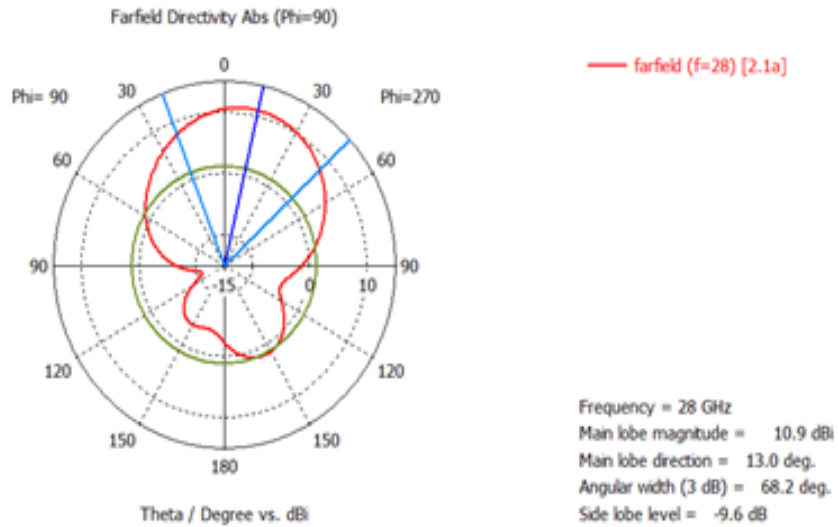


Figure 5. 18a: 2D Radiation Pattern of Proposed 2x1 array

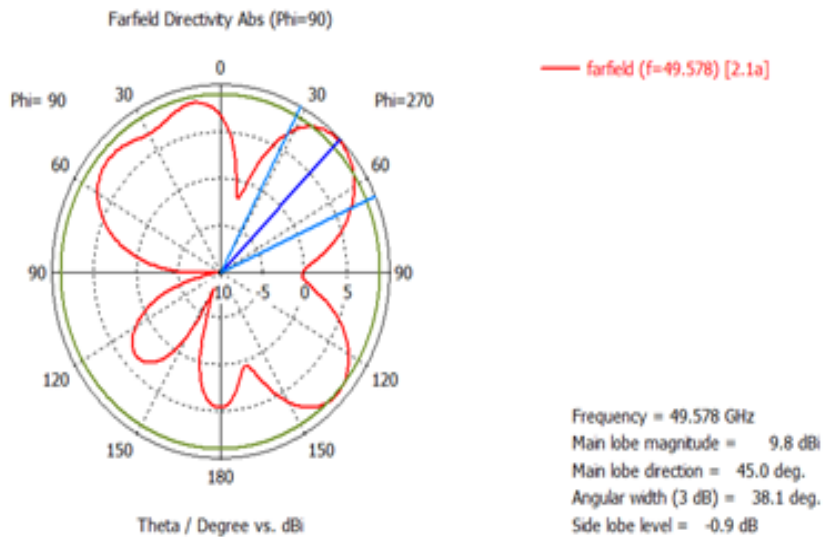


Figure 5.18b: 2D Radiation Pattern of Proposed 2x1 array

5.6: 4x1 slotted antenna arrays

The 4x1 array antenna dual band operation is showed in Figure 5.19. In the first band, a bandwidth of 6.997 GHz was attained, while in the second band, a bandwidth of 12.098 GHz

was reached. The first band's lower frequency is 27.573 GHz, while its higher frequency is 34.57 GHz. The second band, on the other hand, has a lower frequency of 38.938 GHz and a higher frequency of 51.036 GHz. Return losses of -43.056dB at the center frequency of 28.222GHz in the first band and return losses of -35.446dB at the center frequency of 49.578GHz in the second band have been achieved.

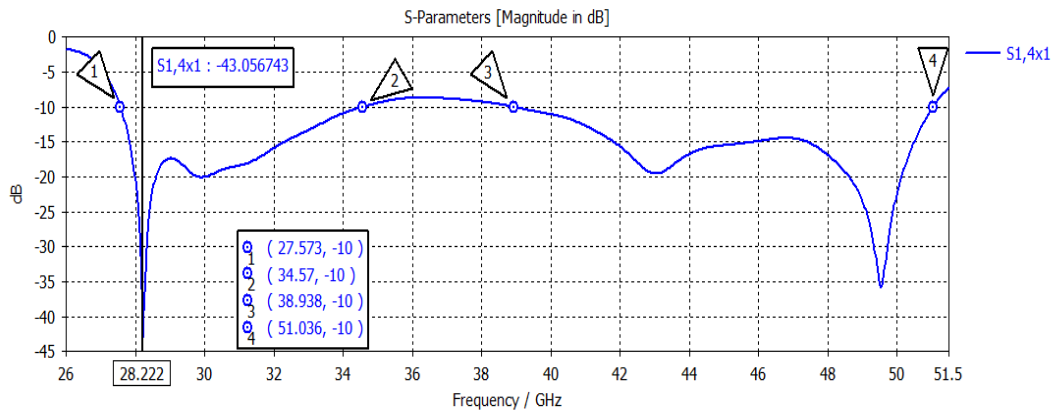


Figure 5. 19: Reflection Coefficient of Proposed 4x1 arrays

The 3D radiation patterns at the center frequencies of 28.222GHz and 49.578GHz are shown in Figures 5.3a and 5.3b respectively. Gains of 12.9dBi and 12.2dBi have been obtained at the center frequencies of 28.222GHz and 49.578GHz respectively.

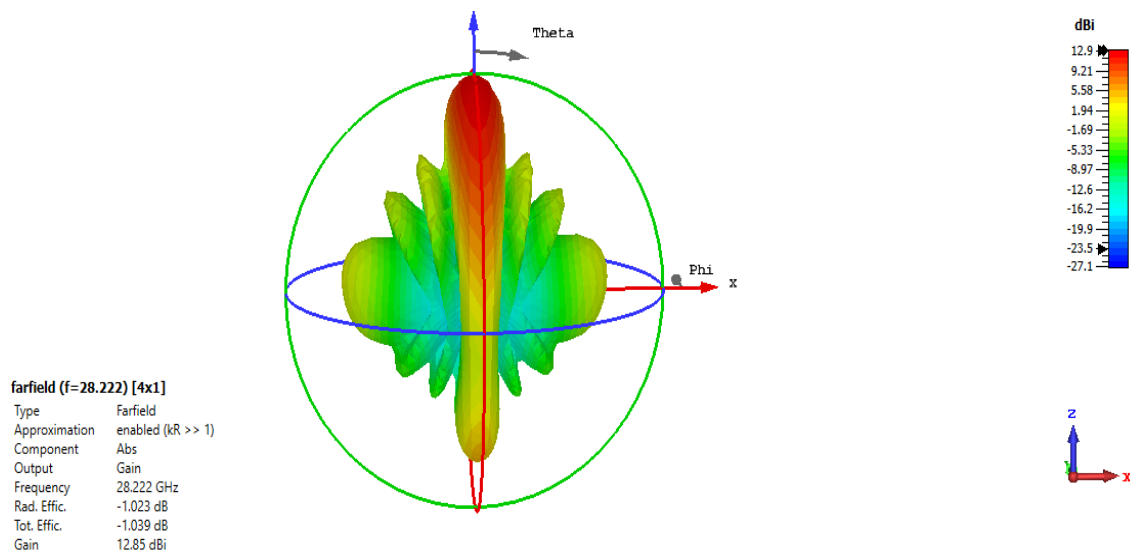


Figure 5. 20a: 3D Radiation Pattern of Proposed 4x1 array

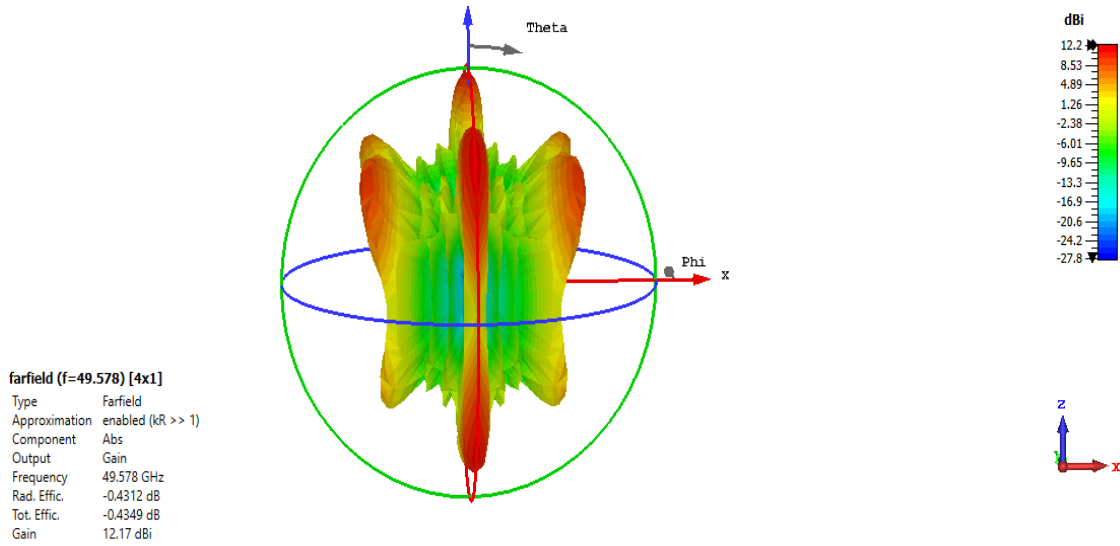


Figure 5.20b: 3D Radiation Pattern of Proposed 4x1 array

The half-power beam widths of 66.8° and 37.7° have been achieved at the center frequencies of 28.222GHz and 49.578GHz, respectively. The side lobe levels of -7.9dB and -1.3dB have been achieved at frequencies of 28GHz and 44.192GHz, respectively. They are observed in these 2D radiation patterns in Figures 5.21a and 5.21b, respectively.

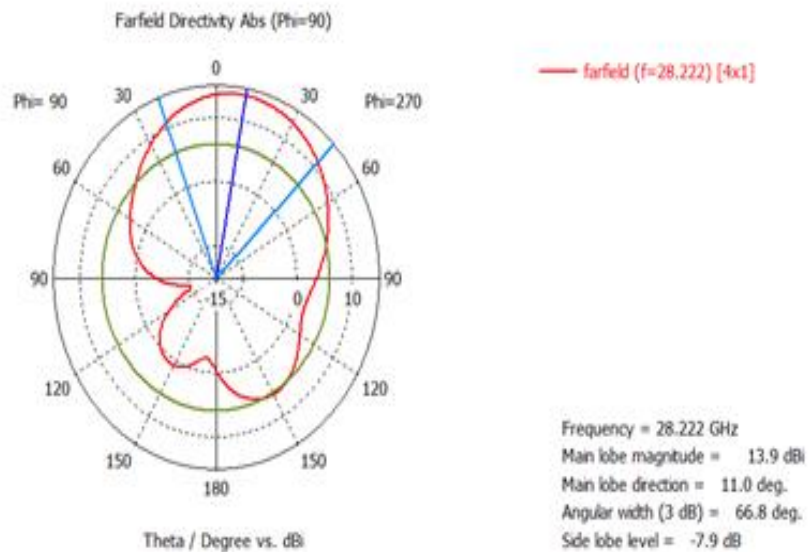


Figure 5. 21b: 2D Radiation Pattern of Proposed 4x1 array

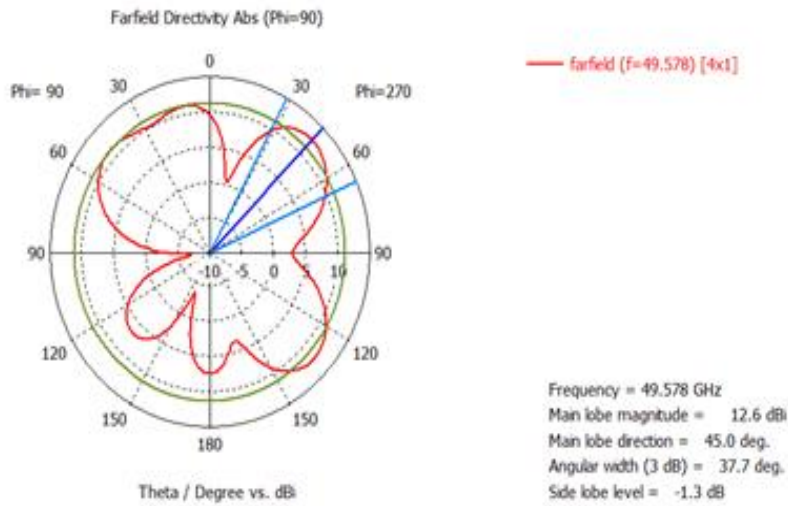


Figure 5.21b: 2D Radiation Pattern of Proposed 4x1 array

5.7 Comparisons between Proposed Antennas and existing Work

Table 5. 1: Comparison of proposed antenna-4 and 4x1 arrays with existing works.

Published antenna	Elements	Center F(GHz)	BW(GHZ)	S11 (dBi)	Gain(dBi)
[13]	1	28	3.9	-35.73	5.54
[33]	1	28	4.1	-42.25	5.61
[34]	1	28	2.48	-39.37	6.37
[35]	1	28	14.674	-40.14	5.29
[36]	1	28.1	1.02	-24.5	8.03
[37]	1	28	Below -10	-30.34	3.75
Proposed Antenna-4	1	28.001	23.858	-46.294	7.27
[20]	4	28	--	-23.6	12.5
[38]	4	29.09	5.2	-18.64	10.8
[39]	4	28	5.47	-32.9	8.85
[40]	4	28	1.45	-21.44	11.23
[41]	4	28	4.127	-31.616	7.8
Proposed Antenna 4x1	4	28.222	6.997	-43.056	12.9

Table 5.1 shows performance comparison of the existing works with the proposed antenna-4 results. The proposed single element design overtakes the designs mentioned in [13, 33, 34, 35, and 37] in terms of beam-gain but it is smaller than the designs reported in [36]. The VSWR of the investigated proposed antenna is minimal, which is significantly closer to ideal values than the designs reported in [13, 33, 34, 35, and 37]. The studied antenna shows minimal return losses at 28 GHz when compared to designs described in [13, 33, 34, 35, 36, and 37]. Finally, the proposed antenna-4 has an ultra-wide bandwidth than the designs described in [13, 33, 34, 35, 36, and 37]. Therefore, the proposed patch antenna gives a highly performance as compared to other similar existing works antennas reported.

Finally, the performance comparison of the existing works with the proposed 4x1 linear antenna results. The return loss, bandwidth, and gain are improved than the other antenna designs. The proposed 4x1arrays antenna also provides the minimal return loss of -43.056dB, better gain of 12.9 dBi and improvement in the bandwidth of 6.994 GHz which is higher than the existing works.

CHAPTER SIX

6. Conclusion and Future work

6.1 Conclusion

This thesis designed, analyzed, and simulated a new slotted microstrip patch antenna for applications. Parametric optimization was also analyzed and discussed for different slot, such as triangular and rectangular slots on the ground plane and circular slots on the radiated patch. The proposed slotted rectangular patch antenna's optimized simulation result obtained a reflection coefficient of -46.294 dB and a VSWR value of 1.009 at 28.001 GHz. The bandwidth obtained was 23.858 GHz, from between 27.412GHz and 51.27GHz, which signified the usability and versatility of the proposed antenna-4. The bandwidth achieved fractional band width was 85.207%, along with a maximum gain of 7.27dBi and a directivity of 7.65dBi. Moreover, the bandwidth performance of the antenna in this work is observed to be suitable for ultra-wideband applications and capable of transferring good quality signals too. The proposed antenna-4 efficiency was 91.62% at 28.001GHz. Also, to increase the antenna gain, we designed antenna arrays based on the single slotted rectangular patch antenna. The proposed 2x1 and 4x1 arrays have a maximum gain of 9.93dBi and 12.9dBi, respectively. The proposed 2x1 and 4x1 arrays of maximum directivity of 10.9 dBi and 14 dBi, respectively. To conclude, the proposed antenna gives to meet the requirements of having an ultra-wide bandwidth, being compact in dimension, having a stable radiation pattern, and having relatively higher gain, which indicates its potential for wireless applications, especially when bandwidth and gain are major concerns.

6.2 Future work

Modifications to the proposed antenna's various regions are advised for further bandwidth increases. For matching, a quarter-wave transformer is designed in between the patch and the feed line has been applied in this work. The employment of other feeding techniques is recommended to investigate the further enhancement of the different characteristics of the proposed antenna. Finally we want recommend; they can carry out the research by increase the array element in order to enhance the performance of the patch antenna.

References

- [1] Simon R. Saunders, "Antennas and Propagation for Wireless Communication Systems", John Wiley & sons, LTD, 2001
- [2] Trevor S. Bird, "Definition and Misuse of Return Loss", IEEE Antennas & Propagation Magazine, vol.51, iss.2, pp.166-167, April 2009.
- [3] Gampala, G., & Reddy, C. J. (2016). Design of millimeter wave antenna arrays for 5G cellular applications using FEKO. 2016 IEEE/ACES International Conference on Wireless Information Technology and Systems (ICWITS) and Applied Computational Electromagnetics (ACES).
- [4] Hong, W., Ko, S.-T., Lee, Y., & Baek, K.-H. (2015). Multi-polarized Antenna Array Configuration for mm-Wave 5G Mobile Terminals. The 2015 International Workshop on Antenna Technology, 60-61.
- [5] Kim, T., Bang, I., & Sung, D. K. (2014). Design Criteria on a mmWave-based Small Cell with Directional Antennas. IEEE 25th International Symposium on Personal, 103-107.
- [6] Balanis, C. (2005). Antenna theory. Hoboken, New Jersey: Wiley
- [7] Andrews, J. G., Buzzi, S., Choi, W., Hanly, S. V., Lozano, A., Soong, A. C., & Zhang, J. C. (2014). What Will 5G Be? IEEE Journal on Selected Areas in Communications, 32(6), 1065-1082.
- [8] Zhao, H., Mayzus, R., Sun, S., Samimi, M., S., J. K., A., . . . T. (2013). 28 GHz Millimeter Wave Cellular Communication Measurements for Reflection and Penetration Loss in and around Buildings in New York City. IEEE International Conference on Communications (ICC), 9-13.
- [9] Alhalabi, R. A. (2010). High Efficiency Planar and RFIC-Based Antennas for Millimeter-WaveCommunication Systems. PHD thesis.
- [10] Lee, J., Song, Y., Choi, E., & Park, J. (2015). mmWave Cellular Mobile Communication for Giga Korea 5G Project. Proceedings of APCC2015 copyright.
- [11] Jamaluddin, M. h., Kamarudin, M., & Khalily, M. (2016). Rectangular Dielectric Resonator Antenna Array for 28 GHz Applications. Progress In Electromagnetics Research, 63,53–61.

- [12] N. Ramli, M. T. Ali, A. L. Yusof, I. Pasya, H. Alias and M. A. Sulaiman, "A Frequency Reconfigurable Stacked Patch Microstrip Antenna (FRSPMA) with aperture coupler technique," 2012IEEE Symposium on Wireless Technology and Applications (ISWTA), Bandung, 2012, pp. 266-271.
- [13] Siju J Thomas, Mehajabeen Fatima, "Bandwidth Improvement of Microstrip Patch Antenna using Partial Ground Plane" International Journal of Engineering Research & Technology (IJERT) ISSN: 2278-0181 Vol. 4 Issue 05, May-2015
- [14] J. Saini and S. K. Agarwal, "T and L slotted patch antenna for future mobile and wireless communication," 2017 8th International Conference on Computing, Communication and Networking Technologies (ICCCNT), Delhi, 2017, pp. 1-5..
- [15] Fan Yang, Xue- Xia Zhang, Xiaoning Ye and YahyaRahmatSamii, "Wide band E-shaped patch antennas for wireless communications" , IEEE Transactions on Antennas and Propagation, vol. 49, pp. 1094-1101, 2001.
- [16] Manoj K. Srivastava, A. K. Gautam and Binod Kumar Kanaujia, "A M- shaped monopole- like slot UWB antenna", Microw. Opt. Technol. Lett., vol. 56, pp. 127-131, 2014.
- [17] Manoj K. Srivastava, A. K. Gautam and Binod Kumar Kanaujia, "A novel A-shaped monopole like slot antenna for ultra wideband applications", Microw. Opt. Technol. Lett., vol. 54, pp. 1826-1829, 2014.
- [18] K. SOLBACH, Microstrip-Franklin antenna , IEEE Trans. Antennas and Propagation, 1982, vol. 30, no. 4, p. 773-775.
- [19] D. Guha, S. Biswas, and Y. M. M. Antar, "Defected Ground Structure for Microstrip Antennas", in Microstrip and Printed Antennas: New Trends, Techniques and Applications, Eds. D. Guha and Y. M. M. Antar, John Wiley & Sons, United Kingdom, 2011.
- [20] Yoshita Gupta , "Stacked Microstrip Patch Antenna with Defected Ground Structures for W-lan and Wimax Applications" Thesis work in Department of Electronics and Communication Engineering, THAPAR UNIVERSITY, PATIALA, June, 2014

- [21] Gurpreet Singh, Rajni, Anupma Marwaha, “Design of G-Shaped Defected Ground Structure for Bandwidth Enhancement”, International Journal of Computer Applications (0975 – 8887) Volume 75– No.9, August 2013.
- [22] Amit Singh Bhadouria, Mithilesh Kumar, “Wide Ku-Band Microstrip Patch Antenna Using Defected patch and ground”, IEEE International Conference on Advances in Engineering & Technology Research (ICAETR - 2014), August 01-02, 2014.
- [23] Adhie Surya Ruswanditya, HeroeWijanto, Yuyu Wahyu. MIMO 8×8 Antenna with Two H-Slotted Rectangular Patch Array for 5G Access Radio at 15 GHz. The IEEE 2017 International Conference on Control, Electronics, Renewable Energy and Communications (ICCEREC), December 2017.
- [24] X. Zhu, J.L. Zhang, T. Cui, Z.q. Zheng, A miniaturized dielectric-resonator phased antenna array with 3D-coverage for 5G mobile terminals, 2018 IEEE 5G World Forum (5GWF), 2018, Page s: 343 – 346.
- [25] Z. U. Khan, Q. H. Abbasi, A. Belenguer, T.H. Loh, A. Alomainy, Hybrid antenna module concept for 28 GHz 5G beam steering cellular devices, 2018 IEEE MTT-S International Microwave Workshop Series on 5G Hardware and System Technologies (IMWS-5G), 2018, Page s: 1 – 3.
- [26] M. Stanley, Y. Huang, H.Y. Wang, H. Zhou, A. Alieldin, S. Joseph, A novel mm-Wave phased array antenna with 360° coverage for 5G smartphone applications, 2017 10th UK-Europe-China Workshop on Millimeter Waves and Terahertz Technologies (UCMMT). 2017, Page s: 1 – 3
- [27] J. Bang, Y. Hong, J. Choi, MM-wave phased array antenna for whole-metal-covered 5G mobile phone applications, 2017 International Symposium on Antennas and propagation (ISAP), 2017, Page s: 1 – 2
- [28] S. F. Jilani, A. Alomainy, Millimeter-wave conformal antenna array for 5G wireless applications, 2017 IEEE International Symposium on Antennas and Propagation & USNC/URSI National Radio Science Meeting, 2017, Page s: 1439 – 1440.
- [29] M. Mantash, T. A. Denidni, Millimeter-wave beam-steering antenna array for 5G applications, 2017 IEEE 28th Annual International Symposium on Personal, Indoor, and Mobile Radio Communications (PIMRC), 2017, Page s: 1 – 3.

- [30] S. S. Zhu, H.W. Liu, Z.J. Chen, P. Wen, A compact gain-enhanced vivaldi antenna array with suppressed mutual coupling for 5G mm-Wave application, *IEEE Antennas and Wireless Propagation Letters*, 2018 , Vol. 17 , No. 5, Page s: 776 – 779
- [31] U. Rafique, H. Khalil, S.U. Rehman, Dual-band microstrip patch antenna array for 5G mobile communications, 2017 Progress in Electromagnetics Research Symposium - Fall (PIERS - FALL), 2017, Page s: 55 – 59.
- [32] K. Klionovski, A. Shamim, M.S. Sharawi, 5G antenna array with wide-angle beam steering and dual linear polarizations, 2017 IEEE International Symposium on Antennas and Propagation & USNC/URSI National Radio Science Meeting, 2017, Page s: 1469 – 1470
- [33] M. J.Ammann and Z. N. Chen, Wideband monopole antennas for multi-band wireless system, *IEEE Antennas Propag. Mag.*, vol. 45, no. 2, pp. 146–150, Apr. 2003.
- [34] J.Luis Arizaca-Cusicuna and M. Clemente-Arenas, "High Gain 4x4Rectangular Patch Antenna Array at 28GHz for Future 5G Applications," 2018 IEEE XXV International Conference on Electronics, Electrical Engineering and Computing (INTERCON), Lima, 2018, pp. 1-4.
- [35] Shehab Khan Noor¹, Nurulazlina Ramli¹, "Compact and Wide Bandwidth Microstrip Patch Antenna for 5G Millimeter Wave Technology: Design and Analysis," 2021 J. Phys.: Conf. 2021.
- [36] Jandi, F. Gharnati and A. Oulad Said, "Design of a compact dual bands patch antenna for 5G applications," 2017 International Conference on Wireless Technologies, Embedded and Intelligent Systems (WITS), Fez, 2017, pp. 1-4,
- [37] Ahmad and W. T. Khan, "Small form factor dual band (28/38 GHz) PIFA antenna for 5G applications," 2017 IEEE MTT-S International Conference on Microwaves for Intelligent Mobility(ICMIM), Nagoya, 2017, pp. 21-24.
- [38] Md. Farid Shah, Aheibam Dinamani Singh "Design and Analysis of Microstrip Patch Antenna Arrays for Millimeter Wave Wireless Communication" (IJEAT) ISSN: 2249 – 8958, Volume-9 Issue-3, February, 2020.

- [39] Janam Maharjan and Dong-You Choi “Four-Element Microstrip Patch Array Antenna with Corporate-Series Feed Network for 5G Communication” International Journal of Antennas and Propagation Volume 2020, Article ID 8760297, 12 pages.
- [40] Mohamed Bakry El Mashade, E. A. Hegazy “Design and Analysis of 28GHz Rectangular Microstrip Patch Array Antenna” WSEAS TRANSACTIONS on COMMUNICATIONS, E-ISSN: 2224-2864, Volume 17, 2018
- [41] Yusnita Rahayu¹, Muhammad Ibnu Hidayat “Design of 28/38 GHz Dual-Band Triangular-Shaped Slot Microstrip Antenna Array for 5G Applications” 2nd International Conference on Telematics and Future Generation Networks, 2018.
- [42] E. G. Cristal, Analysis and exact design of cascaded commensurate transmission-line C-section all-pass networks, IEEE Trans. Microw. Theory Tech., vol. MTT-14, no. 6, pp. 285–291, Jun. 1966.
- [43] S. Gupta, A. Parsa, E. Perret, R. V. Snyder, R. J. Wenzel, and C. Caloz, A Group-delay engineered noncommensurate transmission line all pass network for analog signal processing, IEEE Trans. Microw. Theory Tech., vol. 58, no. 9, pp. 2392–2407, Sep. 2010.
- [44] R.L.Crane, All-pass network synthesis, IEEE Trans. Circuit Theory, vol. 15, no. 4, pp. 474–477, Dec. 1968.
- [45] K. Murase, R. Ishikawa, and K. Honjo, Group delay equalized monolithic microwave integrated circuit amplifier for ultra-wideband based on right/left-handed transmission line design approach, Inst. Elec. Tech. Microw. Ant. Propag., vol. 3, no. 6, pp. 967–973, 2009.
- [46] J. Chen ; Q. Zhang , High scanning-rate periodic leak-wave antennas using complementary microstrip-slotline stubs , 2017 Sixth Asia-Pacific Conference on Antennas and Propagation (APCAP), Year 2017
- [47] <https://lh4.googleusercontent.com/jgjX2n70kheDxzApyB92sd>
- [48] <http://www.henrycountync.com/sitebuilder/images/untitled-512x384.png>
- [49] <http://www.henrycountync.com/sitebuilder/images/untitled-512x384.png>
- [50] <https://qph.ec.quoracdn.net/main-qimg-e4a09518a4f7bd344cba3970559d6e37>

- [51] S. Liao and Q. Xue, Dual Polarized Planar Aperture Antenna on LTCC for 60-GHz Antenna-in-Package Applications, in *IEEE Transactions on Antennas and Propagation*, vol. 65, no. 1, pp. 63-70, Jan. 2017.
- [52] Z. N. Chen, M. Y. W. Chia, *Broadband planar antennas: Design and applications*, 1st Edition. , Chichester, UK: John Wiley & Sons, 2006, p. 243.
- [53] G. R. MacCartney, J. Zhang, S. Nie, T. S. Rappaport, path loss models for 5G millimeter wave propagation channels in urban microcells. , 2013 *IEEE Global Communications Conference (GLOBECOM)*, Exhibition & Industry Forum, 9-13.
- [54] Huang, Y., & Boyle, K. (2008). *Antennas from Theory to Practice*. Chichester: A John Wiley and Sons, Ltd, Publication.
- [55] Stutzman, W., & Thiele, G. (2013). *Antenna theory and design*. John Wiley & Sons, Inc.
- [56] Bevelacqua, P. (2017). *Antenna-theory.com*. (Antenna-Theory.com - Rectangular Microstrip (Patch) Antenna - Feeding Methods) Retrieved from <http://www.antenna-theory.com/antennas/patches/patch3.php>
- [57] Jamaluddin, Kamarudin, & Khalily, *Rectangular Dielectric Resonator Antenna Array for 28 GHz Applications*, 2016
- [58] Garg, Bhartia, Bahl, & Ittipiboon, *Microstrip antenna design handbook*, 2001
- [59] Pan, B. C., Tang, W. X., & Qi, M. Q. (2017). Reduction of the spatially mutual coupling between dual-polarized patch antennas using coupled metamaterial slabs. Retrieved from <http://www.nature.com/articles/srep30288>
- [60] Ghosh¹, J., Ghosal, S., Mitra, D., & Chaudhuri, S. R. (2016). Mutual Coupling Reduction between Closely Placed Microstrip Patch Antenna Using Meander Line Resonator. *Progress In Electromagnetics Research Letters*, 59, 115–122.
- [61] HONG, J.-S., & LANCASTER, M. J. (2001). *Microstrip Filters for RF/Microwave Applications*. NEW YORK / CHICHESTER / WEINHEIM / BRISBANE / SINGAPORE / TORONTO: JOHN WILEY & SONS, INC.
- [62] Jani Ollikainen and Pertti Vainikainen,“Radiation and Bandwidth Characteristics of Two Planar Multistrip Antennas for Mobile Communication Systems”. *IEEE Vehicular Technology Conference Ottawa, Ontario, Canada*. 2: 1186-1190. 1998.

- [63] Al-Hasan, M. J., Denidni, T. A., & Sebak, A. R. (2014). Millimeter-wave Hybrid Isolator for Mutual-Coupling Reduction Applications. 16th International Symposium on Antenna Technology and Applied Electromagnetics (ANTEM), 1-2.
- [64] K., G. C., & Parui, S. K. (2013). Reduction of mutual coupling between E-shaped microstrip antennas by using a simple microstrip I-section. *Microwave and Optical Technology Letters*, 55, 2544–2549.7
- [65] Arya, A. K., Patnaik, A., & Kartikeyan, M. V. (2011). A Compact Array with Low Mutual Coupling using Defected Ground Structures. *IEEE Applied Electromagnetics Conference(AEMC)*, 1-4.
- [66] Salehi, M., Motevasselian, A., Tavakoli, A., & Heidari, a. T. (2006). MUTUAL COUPLING REDUCTION OF MICROSTRIP ANTENNAS USING DEFECTED GROUND STRUCTURE. Iran Telecommunication Research Center (ITRC) for financial support.